Comparing the performance of high-resolution global precipitation products across topographic and climatic gradients of Central Asia

Peña-Guerrero, M. D.[1,2,3,4*], Umirbekov, A.[1,2,3] , Tarasova, L.[4], Müller, D.[1,2,5]

[1] *Leibniz Institute of Agricultural Development in Transition Economies (IAMO), Halle (Saale), Germany*

[2] *Geography Department, Humboldt-Universität zu Berlin, Berlin, Germany*

[3] *Tashkent Institute of Irrigation and Agricultural Mechanization Engineers, Tashkent, Uzbekistan*

[4] *Department of Catchment Hydrology, Helmholtz Centre for Environmental Research, Halle (Saale), Germany*

[5] *Integrative Research Institute on Transformations of Human-Environment System (IRI THESys), Humboldt-Universität zu Berlin, Berlin, Germany*

Correspondence to Mayra Daniela Peña-Guerrero (pena-guerrero@iamo.de)

Umirbekov, A. (Umirbekov@iamo.de)

Tarasova, L. (larisa.tarasova@ufz.de)

Müller, D. (Mueller@iamo.de)

Comparing the performance of high-resolution global precipitation products across topographic and climatic gradients of Central Asia

ABSTRACT

Accurate and reliable precipitation data with high spatial and temporal resolution are essential in studying climate variability, water resources management, and hydrological forecasting. A range of global precipitation data are available to this end, but how well these capture actual precipitation remains unknown, particularly for mountain regions where ground stations are sparse. We examined the performance of three global high-resolution precipitation products for capturing precipitation over Central Asia, a hotspot of climate change, where reliable precipitation data are particularly scarce. Specifically, we evaluated MSWEP, CHIRPS, and GSMAP against independent gauging stations for the period 1985–2015. Our results show that MSWEP and CHIRPS outperformed GSMAP for wetter periods (i.e., winter and spring) and wetter locations (150–600 mm/year), lowlands, mid-altitudes (0–3,000 m), and regions with a winter and spring precipitation regime. MSWEP was best at representing temporal precipitation dynamics, and CHIRPS was most prominent in representing the volume and distribution of precipitation. All products poorly estimated precipitation at higher elevations (>3,000 m), in drier areas (< 150 mm), and in regions characterized by summer precipitation. All precipitation products accurately detected dry spells, but their performance decreased for wet spells with increasing precipitation intensity. In sum, we suggest that CHIRPS and MSWEP provide the most reliable high-resolution precipitation estimates for Central Asia. However, the high spatial and temporal heterogeneity of the performance call for a careful selection of a suitable product for local applications considering the various aspects of precipitation dynamics, climatic, and topographic conditions.

Keywords: Water resources, Turkmenistan, Uzbekistan, Tajikistan, Kazakhstan, Kyrgyzstan, climate change, satellite imagery, validation.

1. INTRODUCTION

The spatial and temporal variability of precipitation shape hydrological cycles (Michaelides et al., 2009). Climate change alters these cycles through changes in precipitation frequency, intensity, and amount and by affecting evapotranspiration patterns (Trenberth, 2011, Tan et al., 2020). These changes in turn impact freshwater availability for agriculture, hydropower, and socioeconomic development (Tan et al., 2020). Most regions with rainfed or irrigated crops depend on precipitation totals during the peak months of plant growth to meet water demand (Funk et al., 2015). Accurate and reliable precipitation records with high spatial and temporal resolutions are therefore essential to study climate variability, the management of water resources, and hydrological forecasting (Sun et al., 2018).

Satellite precipitation sensors are currently the only instruments that can provide near real-time global coverage of precipitation with estimates from geosynchronous infrared sensors on geostationary satellites, which have a high sampling frequency, and polar-orbiting microwave sensors on low Earth–orbiting satellites with lower temporal resolution (Huffman et al., 2007, Maggioni et al., 2016). Satellite-based estimates of precipitation are increasingly used to complement ground station observations, which are limited in areal coverage and density, particularly in inaccessible regions (e.g., mountainous areas), sparsely populated areas, and especially in developing countries (Zambrano-Bigiarini et al., 2017, Sun et al., 2018, Rivera et al., 2018). The lack of station data in mountainous regions is worrisome because precipitation patterns in the mountains are crucial to assess changes in regional climate and in the cryosphere,

which directly affect water availability in downstream regions (Unger-Shayesteh et al., 2013, Immerzeel et al., 2020, Viviroli et al., 2020).

Merging satellite data with gauge measurements from ground stations and reanalysis estimations can improve the accuracy of global precipitation datasets (Tan et al., 2020). Reanalysis-based estimates merge atmospheric measurements and climatic models encompassing physical and dynamical processes to produce consistent, accurate, and continuous meteorological data (Sun et al., 2018, Tan et al., 2020). However, varying availability of ground observations for calibrating the satellite algorithms and reanalysis estimates can compromise the quality of the merged global precipitation datasets (Hu et al., 2018, Zandler et al., 2019, Sun et al., 2018). Therefore, quantitative validation of these global precipitation datasets against ground observations is critical to determine the accuracy and uncertainty of the global products at local and regional scales because misestimations can arise from sampling, instrumental (e.g., sensor observations), and algorithmic errors (Nijssen, 2004, Ebert, 2007, Hu et al., 2018). Validation is hence a keystone for better understanding the impact of climate changes on regional hydrological cycles.

Station data for Central Asia are very scarce, especially in higher elevations and particularly since the dilapidation of much of the meteorological infrastructure following the collapse of the Soviet Union in 1991 and the independence of the Central Asian republics (Schiemann et al., 2008, Unger-Shayesteh et al., 2013). This is unfortunate because precipitation, glaciers, and snowmelt dominate the hydrological budget in the semiarid continental climate of Central Asia, where water fluxes in the mountainous areas play a crucial role in downstream hydrology and water availability (Schär et al., 2004, Mannig et al., 2013, Maussion et al., 2013). The region's economy and ecology heavily rely on water from the two main endorheic rivers, the Amu Darya and Syr Darya, which originate in the headwater catchments of the Pamir and Tien Shan mountains, respectively (Schär et al., 2004, Unger-Shayesteh et al., 2013). In addition, the region is a

hotspot of climate change with warming rates of up to 0.3 °C per decade during the past half century (Teixeira et al., 2013, Reyer et al., 2017, Peng et al., 2019).

Precipitation data sourced from global precipitation products are paramount for data-scarce or ungauged regions, such as Central Asia. Previous studies have evaluated precipitation products for the region with varied and sometimes contrasting results (Table S1). Several studies have suggested that the gauge-based products from the Global Precipitation Climatology Centre (GPCC), with spatial resolutions ranging from 0.25° to 1°, were the most reliable precipitation data for the region but underestimated precipitation in the mountains (Hu et al., 2018, Malsy et al., 2014). In the Amu Darya basin, however, the gauge-based Climate Prediction Center (CPC) (0.5°) dataset performed best (Salehie et al., 2021). In the Pamir mountains, the reanalysis product Modern-Era Retrospective analysis for Research Application (MERRA, 0.5°) stood out, although its performance deteriorated strongly for the period 1998–2012 due to the decline of station data availability (Zandler et al., 2019).

The resolution of the abovementioned gauge-based and reanalysis products is not suitable for studies at regional and catchment scales in Central Asia because their spatial resolution is too coarse to capture precipitation gradients in the complex topography of the region (Hellwig et al., 2018, Henn et al., 2018). Here we evaluate global or near-global precipitation products with a spatial resolution higher than 12 x 12 km and for the period 1981–2015 for the Pamir and Tien Shan mountains and adjacent lowlands of Central Asia. We only selected gauge-corrected products with proven reliability at local and regional scales with a sufficiently long time series available to support analyzing climatic trends and variability (see Table S1 and references therein). Finally, we only consider products that are still operational. These criteria resulted in the selection of the Climate Hazard Group InfraRed Precipitation with Station Data (CHIRPS version 2, 0.05°) (Funk et al., 2015), the Multi-Source Weighted-Ensemble

Precipitation (MSWEP, 0.1°)(Beck et al., 2017a), and the Global Satellite Mapping of Precipitation (GSMAP, 0.1°)(Ushio et al., 2009).

The gauge-corrected versions of GSMAP and MSWEP products were previously considered the best-performing high-resolution precipitation data for the region (Guo et al., 2015, Guo et al., 2017, Lu et al., 2021) and globally (Beck et al., 2017b). The gauge-calibrated CHIRPS product was ranked third in Central Asia when compared to six coarser precipitation products (Salehie et al., 2021). However, the accuracy of MSWEP and CHIRPS has to date not been assessed for Central Asia with data from meteorological stations that were not used for gauge correction of the investigated products.

Here we aim to i) identify the strengths and limitations of the three global precipitation products at daily, monthly, seasonal, and annual timescales, ii) determine the effect of topography and climate regimes on the performance of the precipitation products, iii) quantify the accuracy of the products for different precipitation intensities, and iv), based on these evaluations, propose which precipitation product is most appropriate for subsequent studies. Our analysis hence facilitates informed decisions for assessing climate variability, hydrological and agricultural studies, and water management in this heterogeneous and data-scarce region.

2. STUDY AREA

The study area covers the Tien Shan and Pamir mountains, including the adjacent semi-arid lowlands of Kazakhstan, Kyrgyzstan, Tajikistan, Turkmenistan, and Uzbekistan (Figure 1). In the western and northern Tien Shan and Pamir mountains, most precipitation occurs during the winter and spring seasons (November–March) and falls primarily as snow (Barlow and Tippett, 2008, Sorg et al., 2012). In contrast, parts of central and eastern Tien Shan and eastern Pamir receive most precipitation during summer months (Apel et al., 2018).

Precipitation amounts in the region range from 50 to 1,000 mm annually, primarily determined by orographic uplift and mid-latitude westerly cyclones (Barlow and Tippett, 2008, Mariotti, 2007).

Large-scale variation of extratropical westerlies, which transport moisture from the Atlantic Ocean, the Mediterranean and Caspian Sea, and the Persian Gulf, are the major moisture sources throughout the year in Central Asia; the central and eastern Tien Shan and southeastern Pamir are also affected by the Indian Monsoon in summer (Böhner, 2006, Meier et al., 2013). Moisture fluxes from the Arabian Sea and tropical Africa during warm El Niño Southern Oscillation events cause higher precipitation in autumn and spring in southwestern Central Asia (Mariotti, 2007).

3. DATA

3.1. Precipitation products

3.1.1. CHIRPS

CHIRPS provides daily blended gauge-satellite precipitation estimates covering most global land regions (50° N to 50° S) with a resolution of 0.05° (about 5 km at the equator) from 1981 until present and with a low latency (updated roughly every 2 days, with a stable product released every 3 weeks) (Funk et al., 2015). CHIRPS combines precipitation estimates based on observations of infrared cold cloud duration in which cold and bright clouds are related to convection and therefore rain (Sun et al., 2018). CHIRPS incorporates station data from public data streams and private archives and uses reanalysis-based estimates of the Coupled Forecast System (CFS) to temporally disaggregate from 5-day to daily estimates and when thermal infrared observations are missing (Shukla et al., 2014, Funk et al., 2015). Calibration of CHIRPS involves three main components:

i) the Climate Hazards group Precipitation climatology (CHPclim); ii) the satellite-only Climate Hazards group Infrared Precipitation (CHIRP); and iii) the station-blending procedure (Funk et al., 2015). We downloaded the CHIRPS data from https://data.chc.ucsb.edu/products/CHIRPS-2.0/.

3.1.2. GSMAP

The GSMAP is a multi-satellite algorithm developed by the Japan Science and Technology Agency (Okamoto et al., 2005, Kubota et al., 2007). The algorithm follows three main steps: i) retrieval of precipitation rate from passive microwave data (precipitation-sized particles such as ice content are detected through clouds), provided by the CPC using a Kalman filter approach (Ushio et al., 2009); ii) propagation of the estimated precipitation rates using a backward- and forward-morphing technique (Joyce et al., 2004); and iii) refinement of precipitation data based on the relationship between the infrared brightness temperature and surface precipitation rates (Thiemig et al., 2012). GSMAP has a spatial resolution of 0.1° (about 11 km at the equator) and near-global coverage (60°N to 60°S). It provides hourly averaged rainfall (mm/h). We used daily precipitation values (mm/day) of the GSMAP_Gauge_NRT (near real-time with gauge-calibration using the NOAA CPC Unified Gauge-Based Analysis of Global Precipitation dataset, 0.5°) that has the longest record, starting in 2000 up to present day. We downloaded the GSMAP data from https://sharaku.eorc.jaxa.jp/GSMaP/.

3.1.3. MSWEP

The MSWEP precipitation dataset provides 3-hourly and daily temporal resolution at 0.1° to 0.25° spatial resolutions from 1979 to near present on a global scale (Beck et al., 2017a, Beck et al., 2017b, Beck et al., 2019). It merges gauge observations, satellite, and reanalysis estimates based on timescale and location

(Beck et al., 2019). The weight assigned to the gauge-based estimates is calculated from the gauge network density, and the weights assigned to the satellite- and reanalysis-based estimates are calculated from their comparative performance at surrounding gauges (Sun et al., 2018). We used the latest version of MSWEP with a spatial resolution of 0.1° (about 11 km at the equator). This dataset relies on the reanalysis ERA5, the Multi-Satellite Retrievals from the Global (IMERG) satellite constellation, and the Gridded Satellite (GridSat) thermal infrared imagery, with GridSat only used prior to 2000. Unlike previous versions of MSWEP, this version does not correct underestimation over mountainous and snow-dominated regions in order to match rain gauge observations as closely as possible (Beck, 2021). We downloaded the MSWEP data from http://www.gloh2o.org/.

3.2. Precipitation gauge data

We collected data for 30 stations within the five central Asian countries for the period 1981–2015 (Figure 1), which were not used to correct the global precipitation products. The selection of these stations was based on the list of station names and locations used for the CHIRPS product, the main public gauge sources of MSWEP (Funk et al., 2015). We directly requested and collected the station data from the local research and governmental institutions for validation, and they are not available on open public archiving domains that are used for gauge correction of the global datasets. For some stations, the calibration of the global precipitation made only used a share of the available time series (see Table S2); in these cases, we used only the remaining data for the validation. For GSMAP, we used only the data from those 27 stations, which are available for the period April 2000 through December 2015.

4. METHODS

4.1 Evaluation of precipitation products at different timescales

We evaluated all products at daily, monthly, seasonal, and annual timescales to understand their value for applications that require precipitation data of various temporal resolutions (e.g., hydrological forecasting, water resource management, and agricultural drought monitoring) (Tobin and Bennett, 2014, Funk et al., 2015). For the seasonal timescale, we used calendar seasons: December, January, February (DJF); March, April, May (MAM); June, July, August (JJA); and September, October, November (SON). We grouped stations by elevation bands, precipitation amount, and precipitation regime to evaluate the reliability of precipitation products in diverse environmental conditions and to determine the effect of topography and climate regimes on the performance of the products. Since different precipitation intensities challenge the accuracy of the precipitation estimates, we classified daily precipitation time series into dry spells (<1mm/d) and wet spells of various intensities (1-5mm/d, 5-20mm/d, 20-40mm/d, and >40mm/d) (World Meteorological Organization, 2008, Zambrano-Bigiarini et al., 2017).

4.2 Evaluation of precipitation products at different spatial scales

We performed a point-to-pixel analysis to compare the time series of precipitation gauge data to the corresponding pixel of each product (Thiemig et al., 2012, Zambrano-Bigiarini et al., 2017, Baez-Villanueva et al., 2018). To ensure a consistent comparison among the products, we upscaled CHIRPS to the coarser spatial resolution of MSWEP and GSMAP (i.e., 0.1°) using bilinear interpolation. To determine the effect of the upscaling, we performed the evaluation for both original and upscaled versions (hereafter termed CHIRPS upscaled).

4.3 Evaluation metrics

We evaluated the performance of the products for continuous precipitation time series and for discrete precipitation events. For precipitation time series, we used the modified Kling–Gupta efficiency (KGE') (Gupta et al., 2009, Kling et al., 2012)

(Eq. S1), a dimensionless metric that measures the ability of the precipitation products to reproduce temporal dynamics (correlation coefficient *r*) while preserving the volume (bias ratio β) and the distribution of precipitation (variability ratio γ). KGE', *r*, β, and γ values of 1 indicate a perfect agreement between the precipitation estimates from the product and the ground observations. KGE' values range from $-\infty$ to 1. To determine the product accuracy, we used the mean absolute error (MAE) (Eq. S2), which measures the average magnitude of the difference between the estimated and observed values (Ebert, 2007).

We evaluated the ability of tested precipitation products measuring the correspondence between estimated and observed dry and wet spells of various intensity groups (section 4.1) using a standard contingency table (Ebert, 2007) that summarizes the frequency of correct and false predictions. We used three categorical measures—that is, the probability of detection (POD), the false alarm ratio (FAR), and frequency bias (fBias) (Eq. S3)—that quantify various aspects of performance: POD measures the fraction of correctly identified observed events ("hit rate"), FAR gives the fraction of diagnosed events that were dry spells, and fBias calculates the ratio of the estimated events to the observed precipitation (Ebert, 2007, Baez-Villanueva et al., 2018, Guo et al., 2017). Perfect values are fBias (no bias), POD (detection of all events) is 1, and FAR (no events are incorrectly identified) is 0.

4.4 Dominant precipitation regimes

To capture the heterogeneity of climatic conditions and precipitation seasonality, we determined the precipitation regimes of each gauge and its corresponding grid locations with a monthly sequence of the Pardé coefficients (Pardé, 1933) (Eq. S4), which are dimensionless and can be used for interregional comparisons of precipitation regimes. We used the k-means clustering algorithm (Lloyd, 1982), which minimizes the sum of squares of distances between the gauging stations' values and the cluster with the nearest mean. In that way, we grouped

the "shapes" of the seasonal precipitation regime according to membership in a cluster of precipitation with a similar shape (Weingartner et al., 2013). We selected the optimal number of clusters (k) using the elbow method, a trade-off between the cluster sum of squared errors, and a larger number of clusters (graphically) (Thorndike, 1953, Zhang et al., 2016).

5. RESULTS

5.1 Performance at different timescales

At the seasonal scale, all products performed worst in summer (Figure 2). The overall performance of GSMAP was lower compared to the other products at all timescales, except summer, and especially in winter (KGE'<0). MSWEP, CHIRPS, and its upscaled version showed the best performance in winter. The second-best seasonal performance was spring for MSWEP and autumn for CHIRPS products. All products showed positive correlation coefficients (*r*) for all timescales (Figure S1). MSWEP best captures the temporal dynamics of precipitation in winter, followed by the two CHIRPS products. Moreover, MSWEP and both versions of CHIRPS performed similarly well in autumn and spring. In terms of bias values (β), CHIRPS and CHIRPS upscaled showed the best performance at all timescales, except for the summer season, when it slightly underestimated precipitation (Figure S2). GSMAP revealed higher overestimation in winter and underestimation in summer, whereas MSWEP overestimates precipitation in autumn and summer. Among all products, only GSMAP overestimated the variability (γ) of the observed precipitation, especially in winter (Figure S3), whereas the other products underestimated it at all timescales but particularly during the summer season.

CHIRPS and its upscaled version performed best at monthly timescales and performed similar to MSWEP at the annual timescale. MSWEP showed the highest correlations but also the highest overestimation of precipitation at both scales. CHIRPS upscaled, followed by CHIRPS, performed best in terms of bias

as well as in capturing the precipitation variability at monthly timescales, whereas MSWEP had a better performance in estimating the precipitation variability at the annual timescale.

Our results reveal distinct variations in MAE for different timescales (Figure 3). Regarding the lowest median MAE, both CHIRPS datasets showed it in autumn, GSMAP demonstrated it in summer, and MSWEP showed it in spring and winter. MSWEP in summer and GSMAP in spring, winter, and autumn exhibited the largest errors. CHIRPS products presented the lowest MAE at annual and monthly timescales.

5.2 Spatial evaluation of the products' performance

The highest correlations for all products were found in the western part of the study area, where most of the precipitation occurs in winter and spring (Figure 4). GSMAP overestimated the variability of precipitation (γ) in the southern Pamir and western Tien Shan, while the other products, especially MSWEP, underestimated the variability in this area. All of the datasets overestimated precipitation (β) in the same region, with CHIRPS and its upscaled version performing slightly better. In the southeastern Pamir and western Tien Shan, the overall performance (measured with KGE') was poor for all products, but especially that of GSMAP. The precipitation products performed best in the stations located in the western Pamir and northern Tien Shan, with KGE' values of 0.92 for MSWEP, 0.87 for both CHIRPS products, and 0.83 for GSMAP. Overall, the MAE was lowest in the western region where MSWEP performed best, followed by GSMAP, CHIRPS upscaled, and CHIRPS. We found the highest MAE in the southwestern Tien Shan for all products, followed by the southern Pamir, especially for GSMAP and MSWEP.

To determine how topography and climate regime affected the products' performance, we grouped all stations by elevation bands, precipitation amount, and precipitation regime (Figure 5). All of the products, but especially GSMAP,

had lower performance at high elevations (> 3,000 m). MSWEP performed best in the lowlands (< 1,000 m), while CHIRPS excelled at mid-altitudes (2,000-3,000 m). The MSWEP and CHIRPS products had similar performance between 1,000 m and 2,000 m elevation.

Considering annual precipitation, MSWEP performed best for wetter locations (> 300 mm/year), while both CHIRPS performed best for moderately wet locations (150-300 mm/year) (Figure 5b). For drier locations (< 150 mm/year), all of the products failed to capture the precipitation dynamics. With respect to precipitation regimes, all of the products performed best in cluster 1, where most of the precipitation falls in winter and spring, with long dry summers and autumns (Figure 1). MSWEP showed the highest median values, followed by CHIRPS. In cluster 2, with precipitation in winter and spring but short, dry summers, CHIRPS products performed better than the other products did. However, in cluster 3 (summer precipitation), all of the products performed poorly, and only MSWEP had positive median KGE' values. CHIRPS and its upscaled version were unable to capture the summer precipitation regime of most of the stations (Figure 6 e-f), and MSWEP performed better in representing the region's climatology but overestimated the precipitation amounts.

5.3 Evaluation of dry and wet spells

All of the precipitation products were able to accurately detect dry spells with POD > 0.6 (Figure 7). However, the ability to detect wet spells decreased proportionally with increasing precipitation intensity. MSWEP showed slightly better performance in terms of POD, except for the most intense precipitation class, for which CHIRPS upscaled performed better. The FAR values are consistent with the POD, and all of the products identified dry spells very well, with MSWEP having slightly better performance, which decreased with precipitation intensity, and GSMAP having better performance for moderate precipitation events. CHIRPS showed the closest agreement for all precipitation

intensities in terms of fBias, with a slight overestimation (fBias > 1) of light events and an underestimation (fBias < 1) of heavy precipitation.

6. DISCUSSION

We evaluated the performance of three precipitation products (CHIRPS, GSMAP, and MSWEP) with a spatial resolution higher than 12 km to capture local precipitation patterns over the heterogeneous topography and climate of Central Asia. To do so, we collected precipitation data from 30 independent gauging stations across the region. We accounted for elevation, precipitation regime, precipitation amount, intensity of wet spells, temporal dynamics, and different timescales. Overall, the products all performed best in i) altitudes below 3,000 m; ii) regions dominated by winter and spring precipitation; and iii) wetter periods (i.e., winter and spring) and locations with between 150 and 600 mm of precipitation per year, and the products accurately detected dry spells. We found key differences between the products. MSWEP was best at capturing precipitation dynamics, CHIRPS was best at representing the volume and distribution of precipitation over different timescales and locations, and GSMAP generally showed poorer performance. We also evaluated MSWEP v2.8 for the first time and found that, as compared to previous versions (the results of an earlier evaluation are presented in Figures S4 and S5), v2.8 improved the overall performance in the study region, especially for spring and winter, and did not overestimate precipitation as much.

MSWEP and CHIRPS also captured precipitation dynamics well for the Tibetan Plateau (MSWEP v2) (Liu et al., 2019), Chile (MSWEP v1.1) (Zambrano-Bigiarini et al., 2017), western Africa (MSWEPv2.2) (Satgé et al., 2020), India (MSWEP v2.1) (Prakash, 2019), and the Bolivian Altiplano (MSWEP v2.1) (Satgé et al., 2019). Because CHIRPS is intended to support agricultural drought monitoring, its best performance was expected at around the wettest months for each location (Funk

et al., 2015). This is supported by our results for Central Asia, where CHIRPS performed best for wetter periods and locations. Similar to our results, GSMAP also had the comparatively poor performance for the mountainous endorheic system of the Bolivian Altiplano (Satgé et al., 2019) and for western Africa (Satgé et al., 2020). The accuracy of GSMAP estimates may be affected by the lower number of stations in the source data CPC compared to MSWEP and CHIRPS (Satgé et al., 2020).

Despite MSWEP and CHIRPS having the best overall performance, we found some limitations. Both products performed worst in summer (overestimation of precipitation), during the driest period in areas where winter and spring precipitation dominate (clusters 1 and 2, Figure 1), and for stations in areas with precipitation below 150 mm/year. Similar findings have been reported for CHIRPS in other drylands, such as northeast Brazil (Paredes-Trejo et al., 2017), Sub-Saharan Africa (Harrison et al., 2019), and Mainland China (Bai et al., 2018), as well as for MSWEP (v2.1) in northeast India (Prakash, 2019). The low performance in these areas arguably is due to the very low precipitation, in that a single incorrectly identified rainfall event could lead to 100% over- or underestimation (Zambrano-Bigiarini et al., 2017). Satellite-based precipitation estimates may be more suited to estimating convectional tropical rainfall patterns than the isolated, highly localized, and short-lived convective rainfall typical in semiarid to arid areas (Thiemig et al., 2012, Dinku et al., 2010, Beck et al., 2017b). Our findings support this claim. In dry regions, detecting precipitation is difficult because space-born sensors (e.g., microwave and infrared sensors) can miss the sub-cloud evaporation of raindrops or rainfall suppression by desert aerosols (e.g., mineral dust) and be affected by the land's surface properties, such as a hot background (e.g., upwelling microwave radiation) (Beck et al., 2017b, Dinku et al., 2011).

We found that the products overestimated precipitation at higher elevations (> 3,000 m), possibly because the gauge network density in such areas is low

(Harrison et al., 2019). In complex mountainous terrains, precipitation can be falsely detected due to long-lasting orographic clouds or by the contrast between the temperature and the emissivity of rough land surfaces of water and snow-covered areas, which satellite sensors can misinterpret as precipitation (Satgé et al., 2019, Gebregiorgis and Hossain, 2013, Guo et al., 2015). In addition, in global evaluations, the reanalyses exhibited lower accuracy than the microwave- and infrared-based satellite datasets in the tropics did (Beck et al., 2017b). In contrast, these products perform well in extratropical regions, probably linked to deficiencies in the sub-grid convection parameterization schemes along with issues in the land surface parameterization (Beck et al., 2017b). The coverage of the raw data sources, orographic correction, and interpolation techniques may compromise the accuracy of the precipitation products (Sun et al., 2018). Considering the high dependency of the global precipitation products on local gauge calibration, more efforts are needed to increase the accessibility of local observations in order to improve the products' quality and reliability for hydrological, agricultural, and climate studies.

All of the products performed worse in southeastern Pamir and Tien Shan, where precipitation peaks in summer. Generally, such poor performance among all of the products for summer precipitation can be related to challenges in capturing the orographic uplift of warm clouds, false detection of very cold high clouds as precipitating by infrared products, and microwave products missing warm precipitation from shallow clouds (Behrangi et al., 2014, Gebregiorgis and Hossain, 2013, Satgé et al., 2019). Moreover, for the reanalysis-based products (i.e., CHIRPS and MSWEP), poor summer performance might additionally have resulted from an unrealistic northward displacement of the monsoon cycle (Di Giuseppe et al., 2013) and from the fact that atmospheric models in mid-latitudes can more reliably predict winter precipitation associated with synoptic systems such as fronts than it can summer precipitation, which is more often associated with convective systems such as thunderstorms (Zhu et al., 2014, Haiden et al., 2012).

Although the examined precipitation products were able to detect dry spells accurately, their performance decreased for wet spells as precipitation intensity increased. This lower performance for higher intensities can be associated with local storm events with a spatial extent smaller than the satellites' spatial resolution (Thiemig et al., 2012). The weaker detection ability of CHIRPS might be related to its fixed threshold for detecting precipitation from cloud temperatures that might not be appropriate for this region as well as its dependency on the 0.25° TRMM training data, which contributes to the false detection of rainfall events when averaged over larger areas (Dinku et al., 2010, Paredes-Trejo et al., 2017, Toté et al., 2015, Dinku et al., 2018). The reported duplication and inconsistency in the gauge sources used to calibrate CHIRPS could be additional sources of uncertainty (Rivera et al., 2018).

Finally, our results suggest that the precipitation product's selection depends on the specific user needs or application and the regional characteristics. For example, CHIRPS and MSWEP perform best during winter and spring, which makes them suitable to assess terrestrial water storage prior to the irrigation season. While CHIRPS provides daily precipitation amounts, MSWEP has a higher temporal resolution (3-hour resolution), making it more appropriate for sub-seasonal hydrological monitoring and forecasting (Beck et al., 2017b). Both products have had a long temporal record, from 1979 (MSWEP) and 1981 (CHIRPS) to near the present, with a delay of several days (CHIRPS) or several hours (MSWEP). CHIRPS has a higher spatial resolution (0.05°) as compared to MSWEP (0.1°) and more suitable for smaller catchments in elevations below 3,000 m. The products' best performance was achieved in the western, central, and northern Tien Shan and Pamir mountains and in adjacent regions. Although we did not find considerable differences between the original and upscaled version of CHIRPS, a lower performance of the upscaled version can arise from the resampling method used for upscaling; hence, we advise the use of CHIRPS in its native resolution.

7. CONCLUSION

We presented the first evaluation of three global high-resolution precipitation products over the heterogeneous topography and climate of Central Asia using independent station data. We quantified the products' ability to reproduce temporal dynamics while preserving the volume and distribution of precipitation, evaluated the products' accuracy, and assessed the products' ability to detect dry and wet spells of different intensities accurately.

We found that CHIRPS and MSWEP were the most reliable global products for obtaining high-resolution precipitation estimates in Central Asia, especially for wet seasons. Nevertheless, our results highlight high spatial and temporal heterogeneity of the performance, which indicates that the final product for a local application must be selected with care, based on the guidelines provided above. This is particularly relevant for regions with low precipitation levels and in complex terrain where ground station data are sparse.

Acknowledgments

This research is funded through a doctoral scholarship from the Volkswagenstiftung within the Sustainable Agricultural Development in Central Asia (SUSADICA) project. We would like to thank the Hydrometeorological Service of Tajikistan, Dr. Stephan Weise, Dr. Heiko Apel, Dr. Abror Gafurov, and Dr. Zafar Gafurov for their help in acquiring the station data. The data can be obtained upon reasonable request.

References

ADLER, R. F., SAPIANO, M., HUFFMAN, G. J., WANG, J., GU, G., BOLVIN, D., CHIU, L., SCHNEIDER, U., BECKER, A., NELKIN, E., XIE, P., FERRARO, R. & SHIN, D. B. 2018. The Global Precipitation Climatology Project (GPCP) Monthly Analysis (New Version 2.3) and a Review of 2017 Global Precipitation. *Atmosphere (Basel),* 9.

APEL, H., ABDYKERIMOVA, Z., AGALHANOVA, M., BAIMAGANBETOV, A., GAVRILENKO, N., GERLITZ, L., KALASHNIKOVA, O., UNGER-SHAYESTEH, K., VOROGUSHYN, S. & GAFUROV, A. 2018. Statistical forecast of seasonal discharge in Central Asia using observational records: development of a generic linear modelling tool for operational water resource management. *Hydrology and Earth System Sciences,* 22**,** 2225-2254.

ASHOURI, H., BRAITHWAITE, D. K., SOROOSHIAN, S., HSU, K.-L., KNAPP, K. R., CECIL, L. D., NELSON, B. R. & PRAT, O. P. 2015. PERSIANN-CDR: Daily Precipitation Climate Data Record from Multisatellite Observations for Hydrological and Climate Studies. *Bulletin of the American Meteorological Society,* 96**,** 69-83.

BAEZ-VILLANUEVA, O. M., ZAMBRANO-BIGIARINI, M., RIBBE, L., NAUDITT, A., GIRALDO-OSORIO, J. D. & THINH, N. X. 2018. Temporal and spatial evaluation of satellite rainfall estimates over different regions in Latin-America. *Atmospheric Research,* 213**,** 34-50.

BAI, L., SHI, C., LI, L., YANG, Y. & WU, J. 2018. Accuracy of CHIRPS Satellite-Rainfall Products over Mainland China. *Remote Sensing,* 10.

BARLOW, M. A. & TIPPETT, M. K. 2008. Variability and Predictability of Central Asia River Flows: Antecedent Winter Precipitation and Large-Scale Teleconnections. *Journal of Hydrometeorology,* 9**,** 1334-1349.

BECK, H. E., VAN DIJK, A. I. J. M., LEVIZZANI, V., SCHELLEKENS, J., MIRALLES, D. G., MARTENS, B. & DE ROO, A. 2017a. MSWEP: 3-hourly 0.25° global gridded precipitation (1979–2015) by merging gauge, satellite, and reanalysis data. *Hydrology and Earth System Sciences,* 21**,** 589-615.

BECK, H. E., VERGOPOLAN, N., PAN, M., LEVIZZANI, V., VAN DIJK, A. I. J. M., WEEDON, G. P., BROCCA, L., PAPPENBERGER, F., HUFFMAN, G. J. & WOOD, E. F. 2017b. Global-scale evaluation of 22 precipitation datasets using gauge observations and hydrological modeling. *Hydrology and Earth System Sciences,* 21**,** 6201-6217.

BECK, H. E., WOOD, E. F., PAN, M., FISHER, C. K., MIRALLES, D. G., VAN DIJK, A. I. J. M., MCVICAR, T. R. & ADLER, R. F. 2019. MSWEP V2 Global 3-Hourly 0.1° Precipitation: Methodology and Quantitative Assessment. *Bulletin of the American Meteorological Society,* 100**,** 473-500.

BECK, H. E., WOOD, E. F., PAN, M., FISHER, C. K., MIRALLES, D. G., VAN DIJK, A. I. J. M., MCVICAR, T. R. & ADLER, R. F. 2021. *MSWEP V2.8 Technical Documentation* [Online]. Available: http://www.gloh2o.org/mswep/ [Accessed 07.04 2021].

BEHRANGI, A., TIAN, Y., LAMBRIGTSEN, B. H. & STEPHENS, G. L. 2014. What does CloudSat reveal about global land precipitation detection by other spaceborne sensors? *Water Resources Research,* 50**,** 4893-4905.

BÖHNER, J. 2006. General climatic controls and topoclimatic variations in Central and High Asia. *Boreas,* 35**,** 279-295.

BROCCA, L., FILIPPUCCI, P., HAHN, S., CIABATTA, L., MASSARI, C., CAMICI, S., SCHÜLLER, L., BOJKOV, B. & WAGNER, W. 2019. SM2RAIN–ASCAT (2007–2018): global daily satellite rainfall data from ASCAT soil moisture observations. *Earth System Science Data,* 11**,** 1583-1601.

DEE, D. P., UPPALA, S. M., SIMMONS, A. J., BERRISFORD, P., POLI, P., KOBAYASHI, S., ANDRAE, U., BALMASEDA, M. A., BALSAMO, G., BAUER, P., BECHTOLD, P., BELJAARS, A. C. M.,

VAN DE BERG, L., BIDLOT, J., BORMANN, N., DELSOL, C., DRAGANI, R., FUENTES, M., GEER, A. J., HAIMBERGER, L., HEALY, S. B., HERSBACH, H., HÓLM, E. V., ISAKSEN, L., KÅLLBERG, P., KÖHLER, M., MATRICARDI, M., MCNALLY, A. P., MONGE-SANZ, B. M., MORCRETTE, J. J., PARK, B. K., PEUBEY, C., DE ROSNAY, P., TAVOLATO, C., THÉPAUT, J. N. & VITART, F. 2011. The ERA-Interim reanalysis: configuration and performance of the data assimilation system. *Quarterly Journal of the Royal Meteorological Society,* 137**,** 553-597.

DI GIUSEPPE, F., MOLTENI, F. & DUTRA, E. 2013. Real-time correction of ERA-Interim monthly rainfall. *Geophysical Research Letters,* 40**,** 3750-3755.

DINKU, T., CECCATO, P. & CONNOR, S. J. 2011. Challenges of satellite rainfall estimation over mountainous and arid parts of east Africa. *International Journal of Remote Sensing,* 32**,** 5965-5979.

DINKU, T., CECCATO, P., CRESSMAN, K. & CONNOR, S. J. 2010. Evaluating Detection Skills of Satellite Rainfall Estimates over Desert Locust Recession Regions. *Journal of Applied Meteorology and Climatology,* 49**,** 1322-1332.

DINKU, T., FUNK, C., PETERSON, P., MAIDMENT, R., TADESSE, T., GADAIN, H. & CECCATO, P. 2018. Validation of the CHIRPS satellite rainfall estimates over eastern Africa. *Quarterly Journal of the Royal Meteorological Society,* 144**,** 292-312.

EBERT, E. E. 2007. Methods for Verifying Satellite Precipitation Estimates. *In:* LEVIZZANI V., B. P., TURK F.J. (ed.) *Measuring Precipitation From Space.* Springer.

EUROPEAN CENTRE FOR MEDIUM-RANGE WEATHER FORECAST 2019. ERA5.

FUNK, C., PETERSON, P., LANDSFELD, M., PEDREROS, D., VERDIN, J., SHUKLA, S., HUSAK, G., ROWLAND, J., HARRISON, L., HOELL, A. & MICHAELSEN, J. 2015. The climate hazards infrared precipitation with stations--a new environmental record for monitoring extremes. *Sci Data,* 2**,** 150066.

GEBREGIORGIS, A. S. & HOSSAIN, F. 2013. Understanding the Dependence of Satellite Rainfall Uncertainty on Topography and Climate for Hydrologic Model Simulation. *IEEE Transactions on Geoscience and Remote Sensing,* 51**,** 704-718.

GIBSON, J. K., KALLBERG, P., UPPALA, S., HERNANDEZ, A., NOMURA, A. & SERRANO, A. 1999. ERA description, Version 2. ERA-15 *In:* ECMWF (ed.) *Project Report Series 1.* Reading, United Kingdom: ECMWF.

GUO, H., BAO, A., LIU, T., KURBAN, A. & DE MAEYER, P. 2017. Systematical evaluation of satellite precipitation estimates over Central Asia using an improved error-component procedure. *Journal of Geophysical Research: Atmospheres,* 122**,** 10906-1927.

GUO, H., CHEN, S., BAO, A., HU, J., GEBREGIORGIS, A., XUE, X. & ZHANG, X. 2015. Inter-Comparison of High-Resolution Satellite Precipitation Products over Central Asia. *Remote Sensing,* 7**,** 7181-7211.

GUPTA, H. V., KLING, H., YILMAZ, K. K. & MARTINEZ, G. F. 2009. Decomposition of the mean squared error and NSE performance criteria: Implications for improving hydrological modelling. *Journal of Hydrology,* 377**,** 80-91.

HAIDEN, T., RICHARDSON, D. S., RODWELL, M. J., OKAGAKI, A., ROBINSON, T. & HEWSON, T. 2012. Intercomparison of Global Model Precipitation Forecast Skill in 2010/11 Using the SEEPS Score. *Monthly Weather Review,* 140**,** 2720-2733.

HARRIS, I., JONES, P. D., OSBORN, T. J. & LISTER, D. H. 2014. Updated high-resolution grids of monthly climatic observations - the CRU TS3.10 Dataset. *International Journal of Climatology,* 34**,** 623-642.

HARRISON, L., FUNK, C. & PETERSON, P. 2019. Identifying changing precipitation extremes in Sub-Saharan Africa with gauge and satellite products. *Environmental Research Letters,* 14.

HELLWIG, J., STAHL, K., ZIESE, M. & BECKER, A. 2018. The impact of the resolution of meteorological data sets on catchment-scale precipitation and drought studies. *International Journal of Climatology,* 38**,** 3069-3081.
HENN, B., NEWMAN, A. J., LIVNEH, B., DALY, C. & LUNDQUIST, J. D. 2018. An assessment of differences in gridded precipitation datasets in complex terrain. *Journal of Hydrology,* 556**,** 1205-1219.
HERSBACH, H., BELL, B., BERRISFORD, P., HOR´ANYI, A., SABATER, J., NICOLAS, J., RADU, R., SCHEPERS, D., SIMMONS, A., SOCI, C. & DEE, D. 2019. Global reanalysis: Goodbye ERAInterim, hello ERA5 *ECMWF Newsletter* 159**,** 17–24.
HSU, K.-L., GAO, X., SOROOSHIAN, S. & GUPTA, H. V. 1997. Precipitation estimation from remotely sensed information using artificial neural networks. *Journal of Applied Meteorology,* 43**,** 1834–1853.
HU, Z., HU, Q., ZHANG, C., CHEN, X. & LI, Q. 2016. Evaluation of reanalysis, spatially interpolated and satellite remotely sensed precipitation data sets in central Asia. *Journal of Geophysical Research: Atmospheres,* 121**,** 5648-5663.
HU, Z., ZHOU, Q., CHEN, X., LI, J., LI, Q., CHEN, D., LIU, W. & YIN, G. 2018. Evaluation of three global gridded precipitation data sets in central Asia based on rain gauge observations. *International Journal of Climatology,* 38**,** 3475-3493.
HUFFMAN, G., BOLVIN, D. & NELKIN, E. 2017. Integrated Multi-satellitE Retrievals for GPM (IMERG) Technical Documentation.
HUFFMAN, G. J., ADLER, R. F., ARKIN, P., CHANG, A. & FERRARO, R. 1997. The Global Precipitation Climatology Project (GPCP) Combined Precipitation Dataset. *Bulletin of the American Meteorological Society,* 78**,** 5-20.
HUFFMAN, G. J., ADLER, R. F., GU, G., NELKIN, E. J., BOLVIN, D. T., GU, G., HONG, Y., BOWMAN, K. P., STOCKER, E. F. & WOLFF, D. B. 2007. The TRMM Multisatellite Precipitation Analysis (TMPA): Quasi-Global, Multiyear, Combined-Sensor Precipitation Estimates at Fine Scales. *Journal of Hydrometeorology,* 8**,** 38-55.
HUFFMAN, G. J. & BOLVIN, D. T. 2018. TRMM and Other Data Precipitation Data Set Documentation.
IMMERZEEL, W. W., LUTZ, A. F., ANDRADE, M., BAHL, A., BIEMANS, H., BOLCH, T., HYDE, S., BRUMBY, S., DAVIES, B. J., ELMORE, A. C., EMMER, A., FENG, M., FERNANDEZ, A., HARITASHYA, U., KARGEL, J. S., KOPPES, M., KRAAIJENBRINK, P. D. A., KULKARNI, A. V., MAYEWSKI, P. A., NEPAL, S., PACHECO, P., PAINTER, T. H., PELLICCIOTTI, F., RAJARAM, H., RUPPER, S., SINISALO, A., SHRESTHA, A. B., VIVIROLI, D., WADA, Y., XIAO, C., YAO, T. & BAILLIE, J. E. M. 2020. Importance and vulnerability of the world's water towers. *Nature,* 577**,** 364-369.
JOYCE, R. J., JANOWIAK, J. E., ARKIN, P. A. & XIE, P. 2004. CMORPH: A Method that Produces Global Precipitation Estimates from Passive Microwave and Infrared Data at High Spatial and Temporal Resolution. *Journal of Hydrometeorology,* 5**,** 487-503.
KALNAY, E., KANAMITSU, M., KISTLER, M., COLLINS, W., DEAVEN, D., GANDIN, D., IREDELL, M., SAHA, S., WHITE, G., WOOLLEN, J., ZHU, Y., CHELLIAH, M., EBISUZAKI, W., HIGGINS, W., JANOWIAK, J., MO, K. C., ROPELEWSKI, C., WANG, J., LEETMAA, A., REYNOLDS, R., JENNE, R. & JOSEPH, D. 1996. The NCEP/NCAR 40-Year Reanalysis Project. *Bulletin of the American Meteorological Society* 77**,** 437–447.
KLING, H., FUCHS, M. & PAULIN, M. 2012. Runoff conditions in the upper Danube basin under an ensemble of climate change scenarios. *Journal of Hydrology,* 424-425**,** 264-277.
KUBOTA, T., SHIGE, S., HASHIZUME, H., AONASHI, K., TAKAHASHI, N., SETO, S., HIROSE, M., TAKAYABU, Y. N., USHIO, T., NAKAGAWA, K., IWANAMI, K., KACHI, M. & OKAMOTO, K. I. 2007. Global Precipitation Map Using Satellite-Borne Microwave Radiometers by the

GSMaP Project: Production and Validation. *IEEE Transactions on Geoscience and Remote Sensing,* 45**,** 2259-2275.
LEGATES, D. R. & WILLMOTT, C. J. 1990. Mean seasonal and spatial variability in gauge-corrected, global precipitation. *International Journal of Climatology,* 10**,** 111-127.
LIU, J., SHANGGUAN, D., LIU, S., DING, Y., WANG, S. & WANG, X. 2019. Evaluation and comparison of CHIRPS and MSWEP daily-precipitation products in the Qinghai-Tibet Plateau during the period of 1981–2015. *Atmospheric Research,* 230.
LLOYD, S. P. 1982. Least squares quantization in PCM. *IEEE Transactions on Information Theory,* 28.
LU, X., TANG, G., LIU, X., WANG, X., LIU, Y. & WEI, M. 2021. The potential and uncertainty of triple collocation in assessing satellite precipitation products in Central Asia. *Atmospheric Research,* 252.
MAGGIONI, V., MEYERS, P. C. & ROBINSON, M. D. 2016. A Review of Merged High-Resolution Satellite Precipitation Product Accuracy during the Tropical Rainfall Measuring Mission (TRMM) Era. *Journal of Hydrometeorology,* 17**,** 1101-1117.
MALSY, M., AUS DER BEEK, T. & FLÖRKE, M. 2014. Evaluation of large-scale precipitation data sets for water resources modelling in Central Asia. *Environmental Earth Sciences,* 73**,** 787-799.
MANNIG, B., MÜLLER, M., STARKE, E., MERKENSCHLAGER, C., MAO, W., ZHI, X., PODZUN, R., JACOB, D. & PAETH, H. 2013. Dynamical downscaling of climate change in Central Asia. *Global and Planetary Change,* 110**,** 26-39.
MARIOTTI, A. 2007. How ENSO impacts precipitation in southwest central Asia. *Geophysical Research Letters,* 34.
MAUSSION, F., SCHERER, D., MÖLG, T., COLLIER, E., CURIO, J. & FINKELNBURG, R. 2013. Precipitation Seasonality and Variability over the Tibetan Plateau as Resolved by the High Asia Reanalysis*. *Journal of Climate,* 27**,** 1910-1927.
MEGA, T., USHIO, T., KUBOTA, T., KACHI, M. & AONASHI, K. S., S. Gauge adjusted global satellite mapping of precipitation (GSMaP_Gauge). XXXIth URSI General Assembly and Scientific Symposium (URSI GASS), 16–23 August 2014 2014 Beijing, China. 1-4.
MEIER, C., KNOCHE, M., MERZ, R. & WEISE, S. M. 2013. Stable isotopes in river waters in the Tajik Pamirs: regional and temporal characteristics. *Isotopes Environ Health Stud,* 49**,** 542-54.
MICHAELIDES, S., LEVIZZANI, V., ANAGNOSTOU, E., BAUER, P., KASPARIS, T. & LANE, J. E. 2009. Precipitation: Measurement, remote sensing, climatology and modeling. *Atmospheric Research,* 94**,** 512-533.
MITCHELL, T. D. & JONES, P. D. 2005. An improved method of constructing a database of monthly climate observations and associated high-resolution grids. *International Journal of Climatology,* 25**,** 693-712.
NIJSSEN, B. 2004. Effect of precipitation sampling error on simulated hydrological fluxes and states: Anticipating the Global Precipitation Measurement satellites. *Journal of Geophysical Research,* 109.
OKAMOTO, K. I., USHIO, T., IGUCHI, T., TAKAHASHI, N. & IWANAMI, K. The global satellite mapping of precipitation (GSMaP) project. IEEE International Geoscience and Remote Sensing Symposium, 2005 Seoul. 3414-3416.
PARAJKA, J., MERZ, R., SZOLGAY, J., BLÖSCHL, G., KOHNOVA, S. & HLAVČOVÁ, K. 2008. A Comparison of Precipitation and Runoff Seasonality in Slovakia and Austria. *Meteorologický časopis,* 11**,** 9-14.
PARDÉ, M. 1933. *Fleuves et Rivières,* Paris, Armand Colin.

PAREDES-TREJO, F. J., BARBOSA, H. A. & LAKSHMI KUMAR, T. V. 2017. Validating CHIRPS-based satellite precipitation estimates in Northeast Brazil. *Journal of Arid Environments,* 139**,** 26-40.

PENG, D., ZHOU, T., ZHANG, L. & ZOU, L. 2019. Detecting human influence on the temperature changes in Central Asia. *Climate Dynamics,* 53**,** 4553-4568.

PRAKASH, S. 2019. Performance assessment of CHIRPS, MSWEP, SM2RAIN-CCI, and TMPA precipitation products across India. *Journal of Hydrology,* 571**,** 50-59.

REICHLE, R. H., LIU, Q., KOSTER, R. D., DRAPER, C. S., MAHANAMA, S. P. P. & PARTYKA, G. S. 2017. Land Surface Precipitation in MERRA-2. *Journal of Climate,* 30**,** 1643-1664.

REYER, C. P. O., OTTO, I. M., ADAMS, S., ALBRECHT, T., BAARSCH, F., CARTSBURG, M., COUMOU, D., EDEN, A., LUDI, E., MARCUS, R., MENGEL, M., MOSELLO, B., ROBINSON, A., SCHLEUSSNER, C.-F., SERDECZNY, O. & STAGL, J. 2017. Climate change impacts in Central Asia and their implications for development. *Regional Environmental Change,* 17**,** 1639-1650.

RIENECKER, M. M., WOOLLEN, J., SIENKIEWICZ, M., RUDDICK, A. G., ROBERTSON, F. R., REICHLE, R., REDDER, C. R., PEGION, P., PAWSON, S., OWENS, T., MOLOD, A., LUCCHESI, R., KOSTER, R. D., JOINER, J., GU, W., DA SILVA, A., CONATY, A., COLLINS, D., CHEN, J., BLOOM, S., KIM, G.-K., TAKACS, L., SCHUBERT, S. D., BOSILOVICH, M. G., LIU, E., BACMEISTER, J., TODLING, R., GELARO, R. & SUAREZ, M. J. 2011. MERRA: NASA's Modern-Era Retrospective Analysis for Research and Applications. *Journal of Climate,* 24**,** 3624-3648.

RIVERA, J. A., MARIANETTI, G. & HINRICHS, S. 2018. Validation of CHIRPS precipitation dataset along the Central Andes of Argentina. *Atmospheric Research,* 213**,** 437-449.

SAHA, S., MOORTHI, S., PAN, H.-L., WU, X., WANG, J., NADIGA, S., TRIPP, P., KISTLER, R., WOOLLEN, J., BEHRINGER, D., LIU, H., STOKES, D., GRUMBINE, R., GAYNO, G., WANG, J., HOU, Y.-T., CHUANG, H.-Y., JUANG, H.-M. H., SELA, J., IREDELL, M., TREADON, R., KLEIST, D., VAN DELST, P., KEYSER, D., DERBER, J., EK, M., MENG, J., WEI, H., YANG, R., LORD, S., VAN DEN DOOL, H., KUMAR, A., WANG, W., LONG, C., CHELLIAH, M., XUE, Y., HUANG, B., SCHEMM, J.-K., EBISUZAKI, W., LIN, R., XIE, P., CHEN, M., ZHOU, S., HIGGINS, W., ZOU, C.-Z., LIU, Q., CHEN, Y., HAN, Y., CUCURULL, L., REYNOLDS, R. W., RUTLEDGE, G. & GOLDBERG, M. 2010. The NCEP Climate Forecast System Reanalysis. *Bulletin of the American Meteorological Society,* 91**,** 1015-1058.

SALEHIE, O., ISMAIL, T., SHAHID, S., AHMED, K., ADARSH, S., ASADUZZAMAN, M. & DEWAN, A. 2021. Ranking of gridded precipitation datasets by merging compromise programming and global performance index: a case study of the Amu Darya basin. *Theoretical and Applied Climatology,* 144**,** 985-999.

SATGÉ, F., DEFRANCE, D., SULTAN, B., BONNET, M.-P., SEYLER, F., ROUCHÉ, N., PIERRON, F. & PATUREL, J.-E. 2020. Evaluation of 23 gridded precipitation datasets across West Africa. *Journal of Hydrology,* 581.

SATGÉ, F., RUELLAND, D., BONNET, M.-P., MOLINA, J. & PILLCO, R. 2019. Consistency of satellite-based precipitation products in space and over time compared with gauge observations and snow- hydrological modelling in the Lake Titicaca region. *Hydrology and Earth System Sciences,* 23**,** 595-619.

SCHÄR, C., VASILINA, L., PERTZIGER, F. & DIRREN, S. 2004. Seasonal Runoff Forecasting Using Precipitation from Meteorological Data Assimilation Systems. *Journal of Hydrometeorology,* 5**,** 959-973.

SCHIEMANN, R., LÜTHI, D., VIDALE, P. L. & SCHÄR, C. 2008. The precipitation climate of Central Asia—intercomparison of observational and numerical data sources in a remote semiarid region. *International Journal of Climatology,* 28**,** 295-314.

764 SCHNEIDER, U., BECKER, A., FINGER, P., MEYER-CHRISTOFFER, A., RUDOLF, B. & ZIESE, M. 2011.
765 GPCC Full Data Reanalysis Version 6.0 at 0.5°: Monthly Land-Surface Precipitation from
766 Rain-Gauges built on GTS-based and Historic Data.
767 SCHNEIDER, U., BECKER, A., FINGER, P., MEYER-CHRISTOFFER, A. & ZIESE, M. 2015. GPCC full
768 data reanalysis version 7.0 at 0.5°: monthly land-surface precipitation from rain-gauges
769 built on GTS-based and historic data. 7 ed.
770 SCHNEIDER, U., BECKER, A., FINGER, P., MEYER-CHRISTOFFER, A. & ZIESE, M. 2018a. GPCC Full
771 Data Monthly Product Version 2018 at 0.25°: Monthly Land-Surface Precipitation from
772 Rain-Gauges built on GTS-based and Historical Data.
773 SCHNEIDER, U., BECKER, A., FINGER, P., MEYER-CHRISTOFFER, A. & ZIESE, M. 2018b. GPCC
774 Monitoring Product Version 6: Near Real-Time Monthly Land-Surface Precipitation
775 from Rain-Gauges based on SYNOP and CLIMAT data.
776 SHUKLA, S., MCNALLY, A., HUSAK, G. & FUNK, C. 2014. A seasonal agricultural drought forecast
777 system for food-insecure regions of East Africa. *Hydrology and Earth System Sciences,*
778 18**,** 3907-3921.
779 SORG, A., BOLCH, T., STOFFEL, M., SOLOMINA, O. & BENISTON, M. 2012. Climate change
780 impacts on glaciers and runoff in Tien Shan (Central Asia). *Nature Climate Change,* 2**,**
781 725-731.
782 SOROOSHIAN, S., HSU, K.-L., GAO, X., GUPTA, H. V., IMAM, B. & BRAITHWAITE, D. 2000.
783 Evaluation of PERSIANN system satellite-based estimates of tropical rainfall. *Bulletin of*
784 *the American Meteorological Society,* 81**,** 2035–2046.
785 SUN, Q., MIAO, C., DUAN, Q., ASHOURI, H., SOROOSHIAN, S. & HSU, K. L. 2018. A Review of
786 Global Precipitation Data Sets: Data Sources, Estimation, and Intercomparisons.
787 *Reviews of Geophysics,* 56**,** 79-107.
788 TAN, X., WU, Y., LIU, B. & CHEN, S. 2020. Inconsistent changes in global precipitation
789 seasonality in seven precipitation datasets. *Climate Dynamics,* 54**,** 3091-3108.
790 TEIXEIRA, E. I., FISCHER, G., VAN VELTHUIZEN, H., WALTER, C. & EWERT, F. 2013. Global hot-
791 spots of heat stress on agricultural crops due to climate change. *Agricultural and*
792 *Forest Meteorology,* 170**,** 206-215.
793 THIEMIG, V., ROJAS, R., ZAMBRANO-BIGIARINI, M., LEVIZZANI, V. & DE ROO, A. 2012.
794 Validation of Satellite-Based Precipitation Products over Sparsely Gauged African River
795 Basins. *Journal of Hydrometeorology,* 13**,** 1760-1783.
796 THORNDIKE, R. L. 1953. Who belongs in the family? *Psychometrika,* 18**,** 267-276.
797 TOBIN, K. J. & BENNETT, M. E. 2014. Satellite precipitation products and hydrologic
798 applications. *Water International,* 39**,** 360-380.
799 TOTÉ, C., PATRICIO, D., BOOGAARD, H., VAN DER WIJNGAART, R., TARNAVSKY, E. & FUNK, C.
800 2015. Evaluation of Satellite Rainfall Estimates for Drought and Flood Monitoring in
801 Mozambique. *Remote Sensing,* 7**,** 1758-1776.
802 TRENBERTH, K. E. 2011. Changes in precipitation with climate change. *Climate Research,* 47**,**
803 123-138.
804 UNGER-SHAYESTEH, K., VOROGUSHYN, S., FARINOTTI, D., GAFUROV, A., DUETHMANN, D.,
805 MANDYCHEV, A. & MERZ, B. 2013. What do we know about past changes in the water
806 cycle of Central Asian headwaters? A review. *Global and Planetary Change,* 110**,** 4-25.
807 UPPALA, S. M., KÅLLBERG, P. W., SIMMONS, A. J., ANDRAE, U., BECHTOLD, V. D. C., FIORINO,
808 M., GIBSON, J. K., HASELER, J., HERNANDEZ, A., KELLY, G. A., LI, X., ONOGI, K.,
809 SAARINEN, S., SOKKA, N., ALLAN, R. P., ANDERSSON, E., ARPE, K., BALMASEDA, M. A.,
810 BELJAARS, A. C. M., BERG, L. V. D., BIDLOT, J., BORMANN, N., CAIRES, S., CHEVALLIER,
811 F., DETHOF, A., DRAGOSAVAC, M., FISHER, M., FUENTES, M., HAGEMANN, S., HÓLM,
812 E., HOSKINS, B. J., ISAKSEN, L., JANSSEN, P. A. E. M., JENNE, R., MCNALLY, A. P.,
813 MAHFOUF, J. F., MORCRETTE, J. J., RAYNER, N. A., SAUNDERS, R. W., SIMON, P., STERL,

A., TRENBERTH, K. E., UNTCH, A., VASILJEVIC, D., VITERBO, P. & WOOLLEN, J. 2005. The ERA-40 re-analysis. *Quarterly Journal of the Royal Meteorological Society,* 131**,** 2961-3012.

USHIO, T., SASASHIGE, K., KUBOTA, T., SHIGE, S., OKAMOTO, K. I., AONASHI, K., INOUE, T., TAKAHASHI, N., IGUCHI, T., KACHI, M., OKI, R., MORIMOTO, T. & KAWASAKI, Z.-I. 2009. A Kalman Filter Approach to the Global Satellite Mapping of Precipitation (GSMaP) from Combined Passive Microwave and Infrared Radiometric Data. *Journal of the Meteorological Society of Japan,* 87A**,** 137-151.

VIDALE, P. L., LÜTHI, D., FREI, C., SENEVIRATNE, S. I. & SCHÄR, C. 2003. Predictability and uncertainty in a regional climate model. *Journal of Geophysical Research,* 108.

VIVIROLI, D., KUMMU, M., MEYBECK, M., KALLIO, M. & WADA, Y. 2020. Increasing dependence of lowland populations on mountain water resources. *Nature Sustainability,* 3**,** 917-928.

WEEDON, G. P., BALSAMO, G., BELLOUIN, N., GOMES, S., BEST, M. J. & VITERBO, P. 2014. The WFDEI meteorological forcing data set: WATCH Forcing Data methodology applied to ERA-Interim reanalysis data. *Water Resources Research,* 50**,** 7505-7514.

WEINGARTNER, R., BLÖSCHL, G., HANNAH, D. M., MARKS, D. G., PARAJKA, J., PEARSON, C. S., ROGGER, M., SALINAS, J. L., SAUQUET, E., SRIKANTHAN, R., THOMPSON, S. E., VIGLIONE, A., BLOSCHL, G., SIVAPALAN, M., WAGENER, T., VIGLIONE, A. & SAVENIJE, H. 2013. Prediction of seasonal runoff in ungauged basins. *Runoff Prediction in Ungauged Basins.*

WILLMOTT, C. & MATSUURA, K. 2012. Terrestrial precipitation: 1900–2010 gridded monthly time series (version 3.01), terrestrial air temperature and precipitation: monthly and annual time series (1900–2010).

WORLD METEOROLOGICAL ORGANIZATION 2008. Present and past weather, state of the ground

In: ORGANIZATION, W. M. (ed.) *Guide to meteorological instruments and methods of observation.* Seventh ed. Geneva, Switzerland.

XIE, P., YOO, S.-H., JOYCE, R. & YAROSH, Y. 2014. Bias-corrected CMORPH: A 13-year analysis of high-resolution global precipitation.

YATAGAI, A., KAMIGUCHI, K., ARAKAWA, O., HAMADA, A., YASUTOMI, N. & KITOH, A. 2012. APHRODITE: Constructing a Long-Term Daily Gridded Precipitation Dataset for Asia Based on a Dense Network of Rain Gauges. *Bulletin of the American Meteorological Society,* 93**,** 1401-1415.

ZAMBRANO-BIGIARINI, M., NAUDITT, A., BIRKEL, C., VERBIST, K. & RIBBE, L. 2017. Temporal and spatial evaluation of satellite-based rainfall estimates across the complex topographical and climatic gradients of Chile. *Hydrology and Earth System Sciences,* 21**,** 1295-1320.

ZANDLER, H., HAAG, I. & SAMIMI, C. 2019. Evaluation needs and temporal performance differences of gridded precipitation products in peripheral mountain regions. *Sci Rep,* 9**,** 15118.

ZHANG, Y., MOGES, S. & BLOCK, P. 2016. Optimal Cluster Analysis for Objective Regionalization of Seasonal Precipitation in Regions of High Spatial–Temporal Variability: Application to Western Ethiopia. *Journal of Climate,* 29**,** 3697-3717.

ZHU, H., WHEELER, M. C., SOBEL, A. H. & HUDSON, D. 2014. Seamless Precipitation Prediction Skill in the Tropics and Extratropics from a Global Model. *Monthly Weather Review,* 142**,** 1556-1569.

862 FIGURES

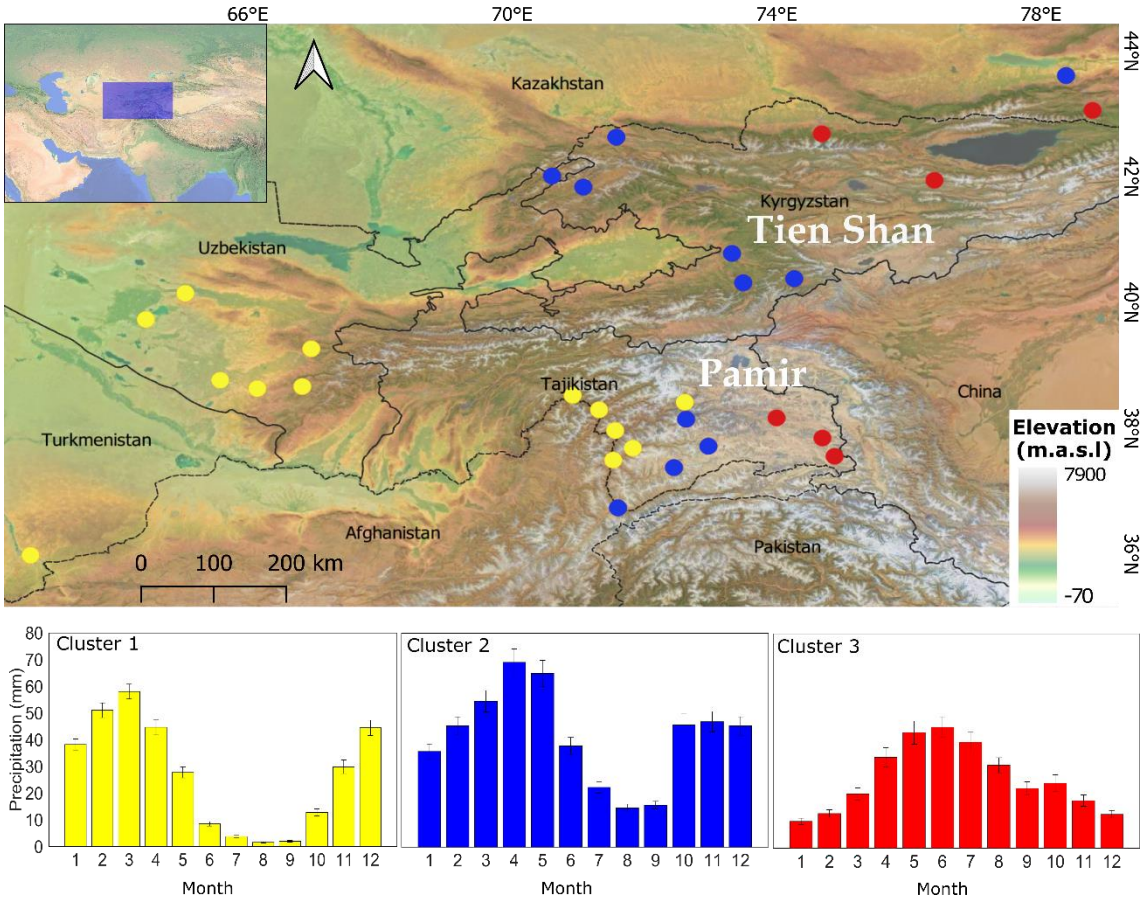

863

864 **Figure 1.** Study area and location of the 30 precipitation stations used for validation. Bar plots
865 represent the annual precipitation regimes (section 4.4) of the clusters shown in the map: Cluster
866 1 (yellow) is characterized by winter and spring precipitation and long, dry summers and
867 autumns; cluster 2 (blue) has winter and spring precipitation and a short, dry summer period;
868 and summer precipitation dominates in cluster 3 (red).

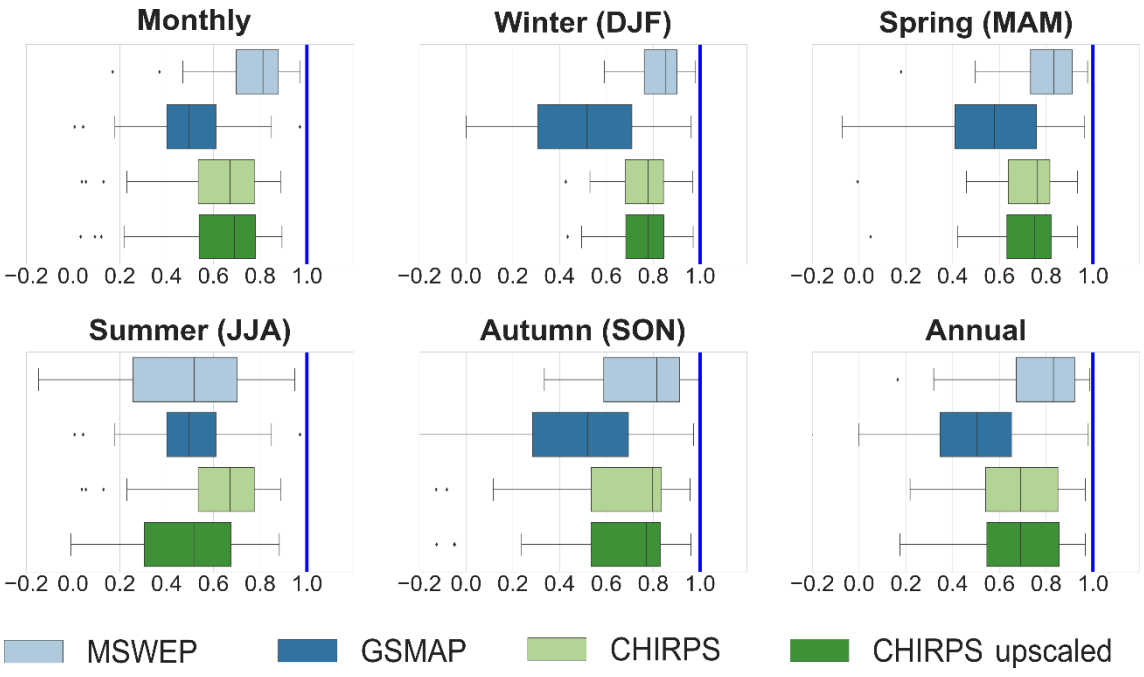

Figure 2. KGE' between the precipitation products and precipitation gauge data for six different timescales. The vertical blue line indicates the optimum value for KGE'. From left to right and up to bottom: monthly, winter (December, January, February), spring (March, April, May), summer (June, July, August), and autumn (September, October, November).

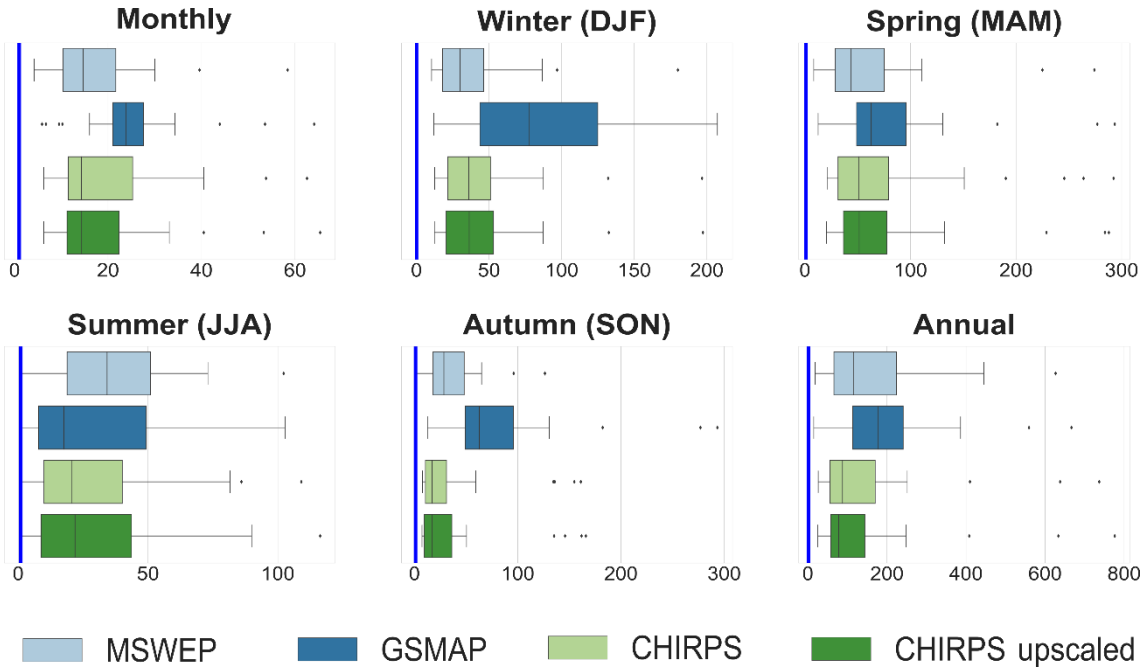

Figure 3. Mean absolute error (MAE) in mm of various global precipitation datasets and precipitation gauge data for six different temporal scales. The vertical blue line indicates the optimum value for MAE.

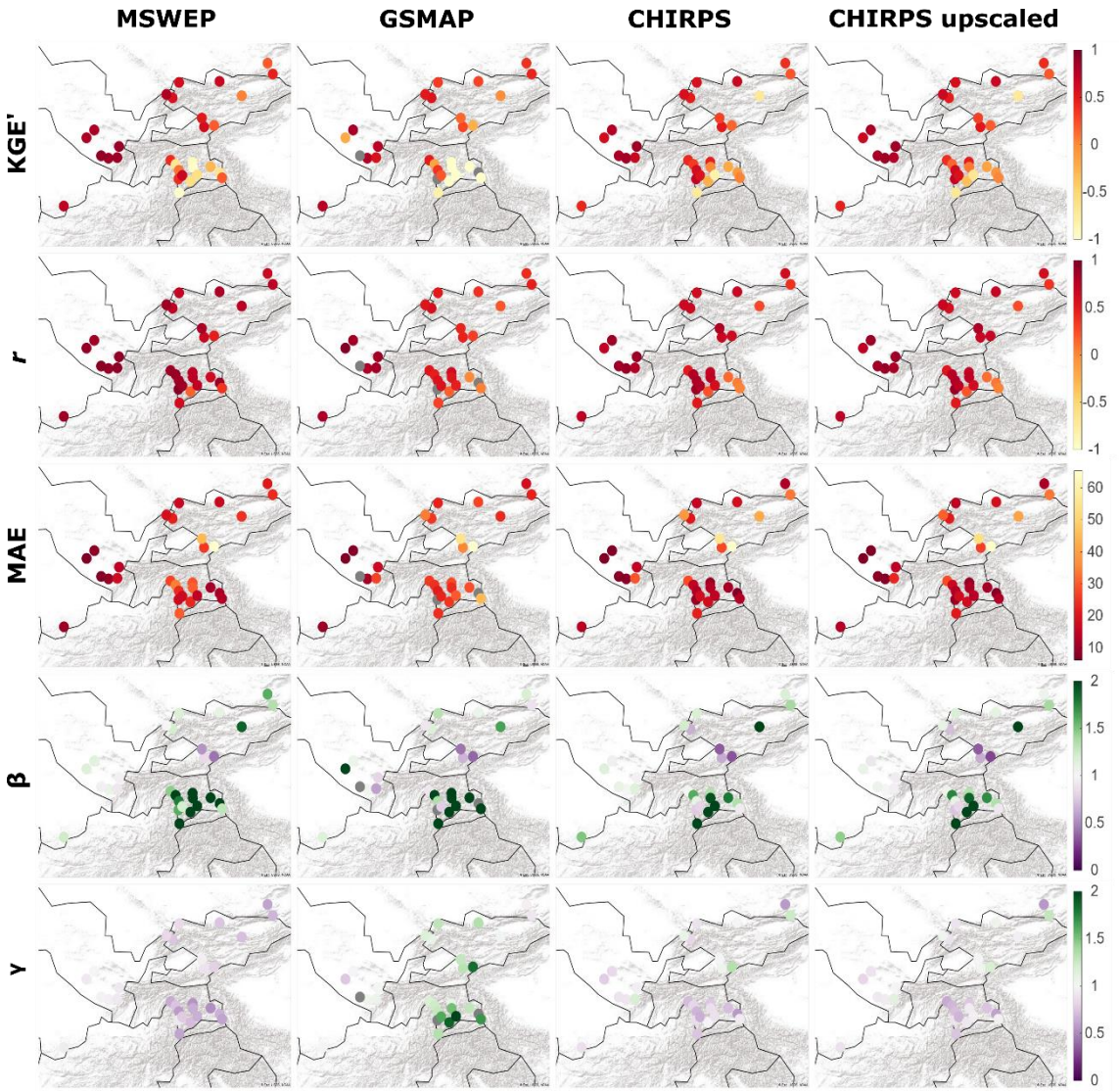

Figure 4. KGE', its components (r, β, γ), and MAE derived from a monthly timescale. The colors for KGE', r, and MAE range from light yellow (very poor performance) to dark red (best performance). For β and γ, white colors represent their best performance, while underestimation is depicted in dark purple and overestimation is depicted in dark green. Gray color identifies stations not available for product evaluation (i.e., GSMAP, data before 2000). The black outlines correspond to the countries (see figure 1 for a detailed map of the region).

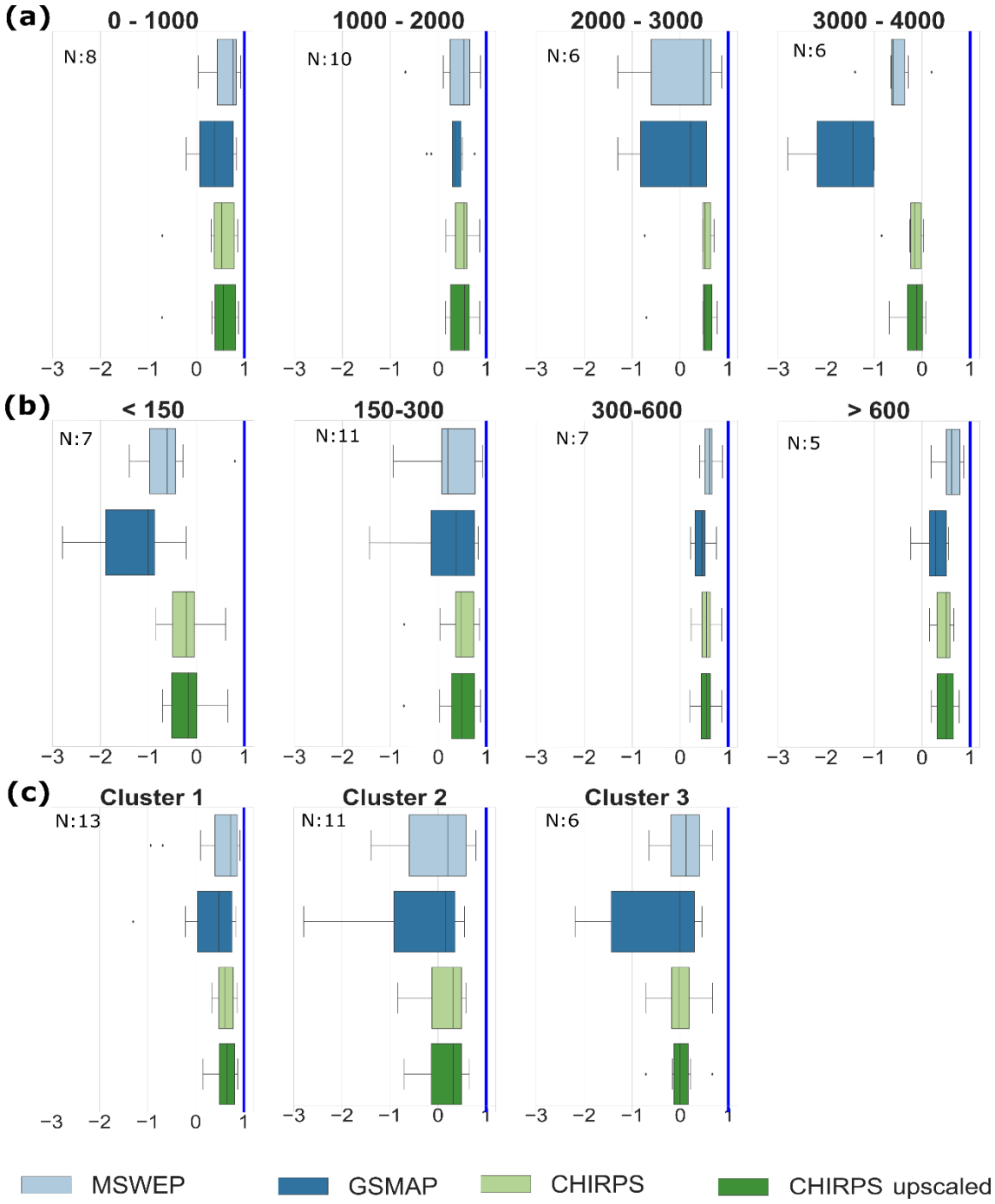

Figure 5. KGE' at a monthly timescale between the precipitation products and precipitation gauge data for different a) elevation bands: 0–1000 m, 1000–2000 m, 2000-3000 m, and 3000-4000 m; b) mean annual precipitation (2000-2015); c) precipitation regimes with corresponding clusters (cluster 1 has winter-spring precipitation, long dry summers; cluster 2 has winter-spring precipitation, short dry summers, and cluster 3 is characterized by summer precipitation). The vertical blue line indicates the optimum value for KGE'. *N* indicates the number of stations in group.

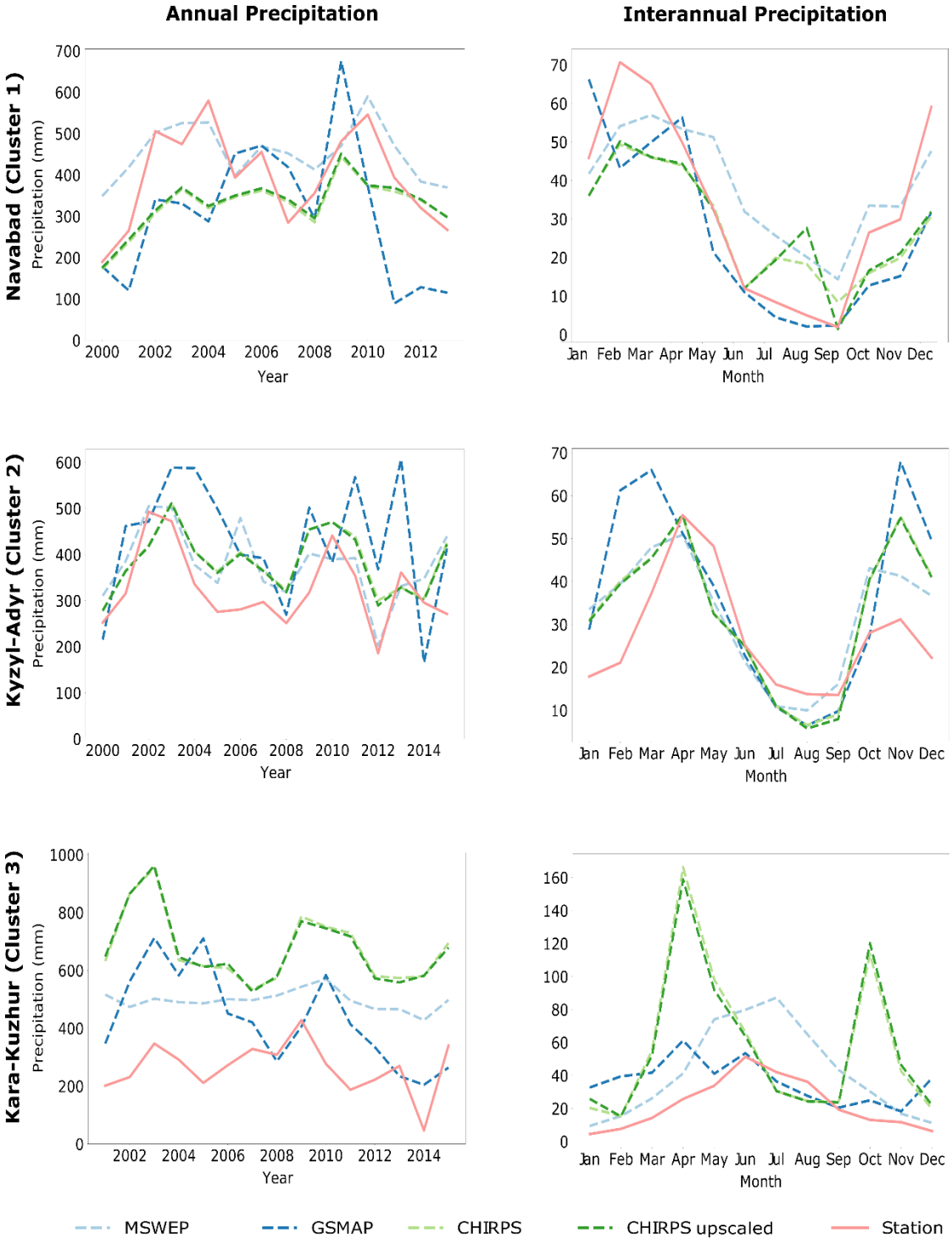

Figure 6. Mean annual precipitation and interannual variation in precipitation estimated by the precipitation products (dashed lines), as compared to the gauging stations (solid lines) for each cluster. Cluster 1 (winter/spring precipitation; long, dry summers); Cluster 2 (winter/spring precipitation; short, dry summers), and Cluster 3 (summer precipitation).

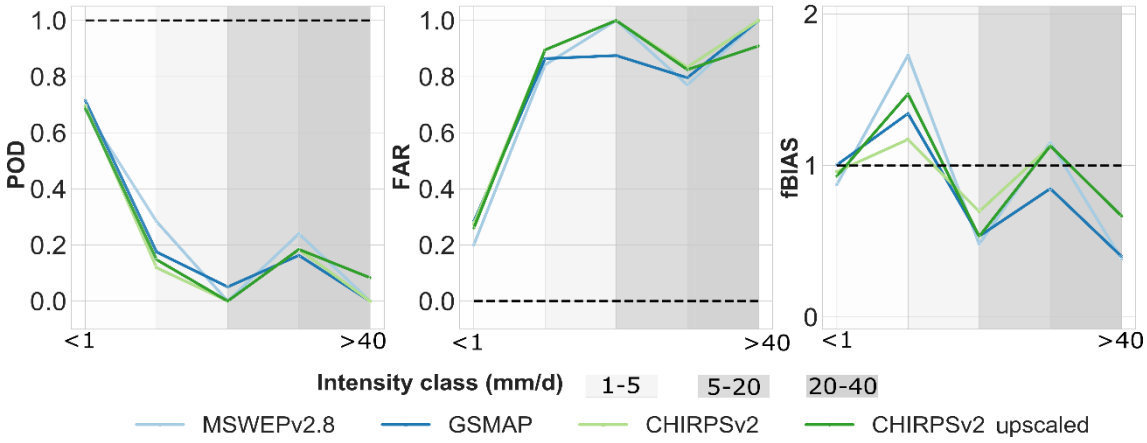

Figure 7. Median values of probability of detection (POD), false alarm ratio (FAR), and frequency of bias (fBias) performance for dry spells (< 1 mm/d) and wet spells of different intensities (1–5 mm/d, 5–20 mm/d, 20–40 mm/d, and > 4 0mm/d). The horizontal dashed line indicates the optimum POD, FAR, and fBIAS values.

Comparing the performance of high-resolution global precipitation products across topographic and climatic gradients of Central Asia

Peña-Guerrero, M. D.[1,2,3,4*], Umirbekov, A.[1,2,3] , Tarasova, L.[4], Müller, D.[1,2,5]

[1] *Leibniz Institute of Agricultural Development in Transition Economies (IAMO), Halle (Saale), Germany*

[2] *Geography Department, Humboldt-Universität zu Berlin, Berlin, Germany*

[3] *Tashkent Institute of Irrigation and Agricultural Mechanization Engineers, Tashkent, Uzbekistan*

[4] *Department of Catchment Hydrology, Helmholtz Centre for Environmental Research, Halle (Saale), Germany*

[5] *Integrative Research Institute on Transformations of Human-Environment System (IRI THESys), Humboldt-Universität zu Berlin, Berlin, Germany*

Correspondence to Mayra Daniela Peña-Guerrero (pena-guerrero@iamo.de)

Umirbekov, A. (Umirbekov@iamo.de)

Tarasova, L. (larisa.tarasova@ufz.de)

Müller, D. (Mueller@iamo.de)

Supporting information

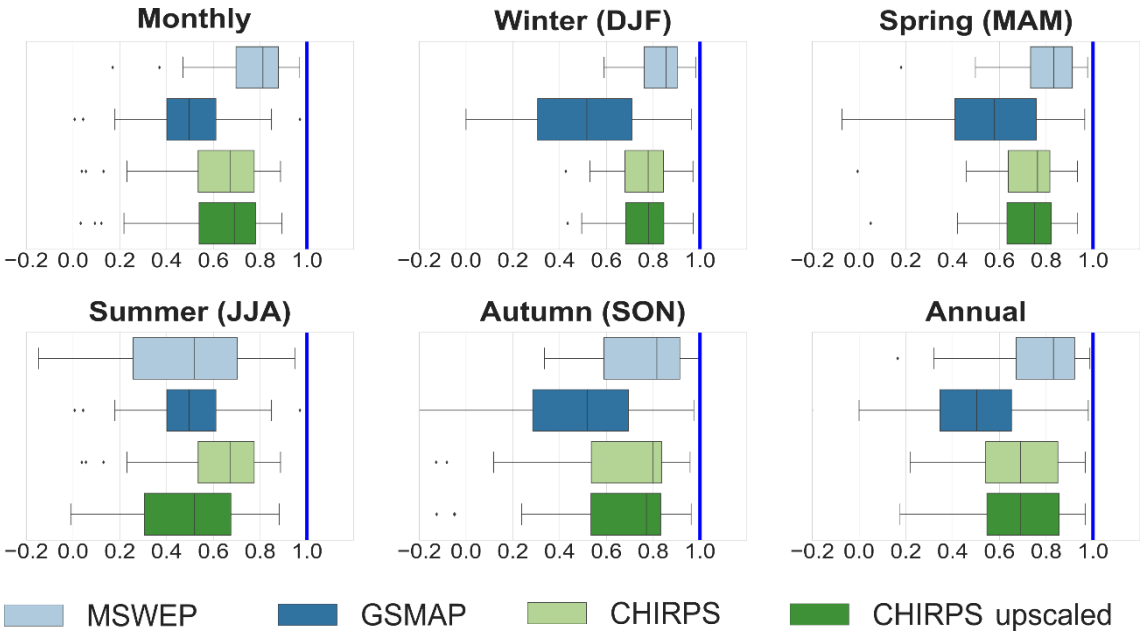

Figure S1. Pearson correlation coefficient (*r*) between different satellite estimations and precipitation gauge data at the corresponding grid cell for six temporal scales. The vertical blue line shows the optimum value for *r*.

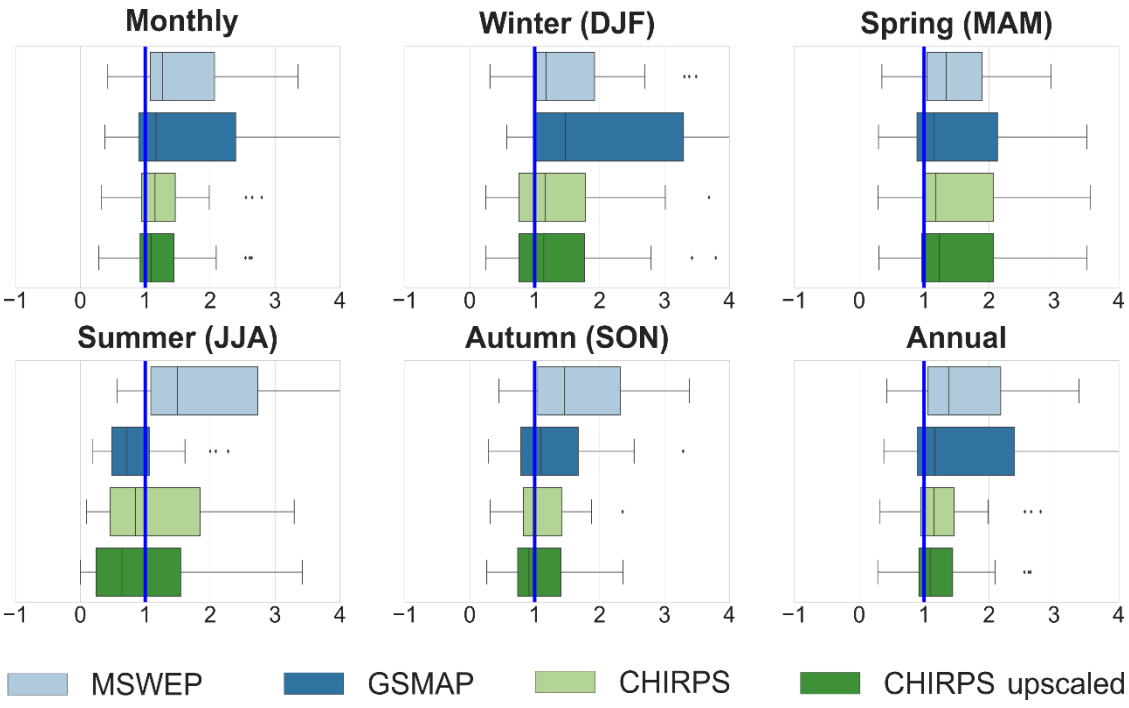

Figure S2. Bias ratio (β) of different satellite estimations and precipitation gauge data at the corresponding grid cell for six temporal scales. The vertical blue line shows the optimum value for β.

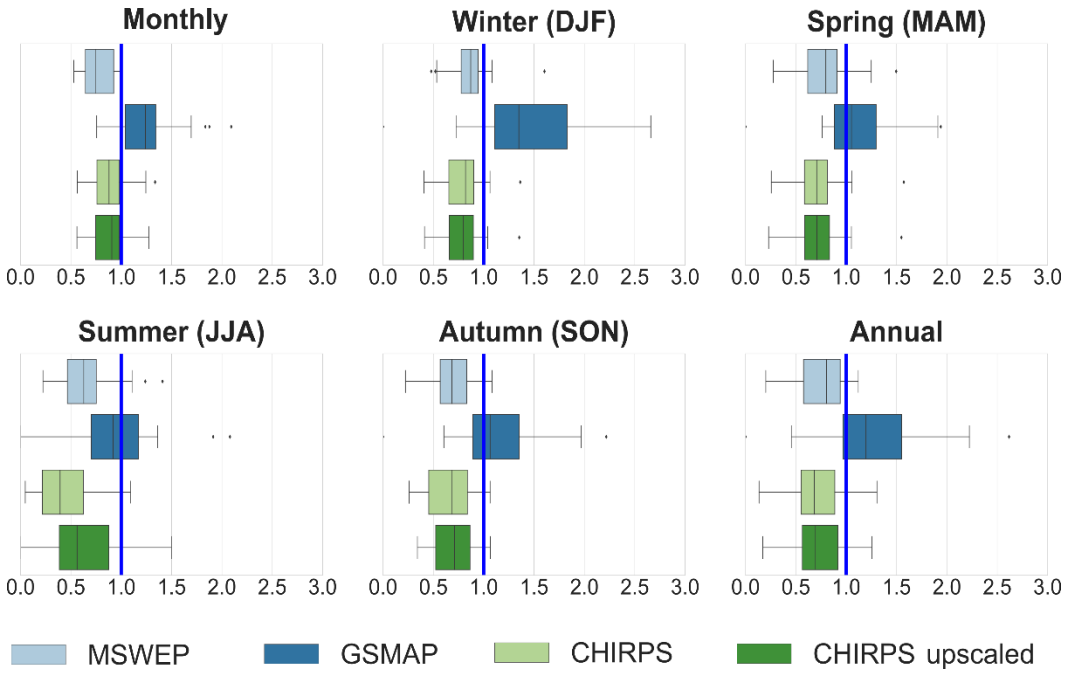

Figure S3. Variability ratio (γ) between different satellite estimations and precipitation gauge data at the corresponding grid cell for six temporal scales. The vertical blue line shows the optimum value for γ.

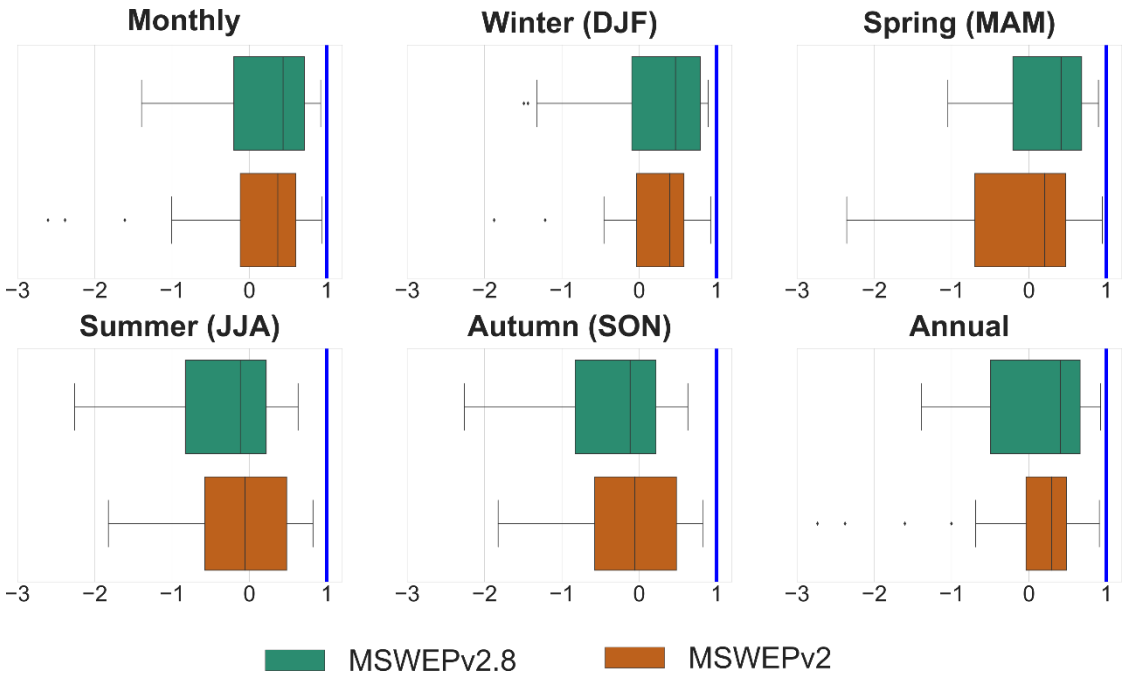

Figure S4. KGE' for both MSWEP versions and precipitation gauge data at the corresponding grid cell for six temporal scales. The vertical blue line shows the optimum value for KGE'.

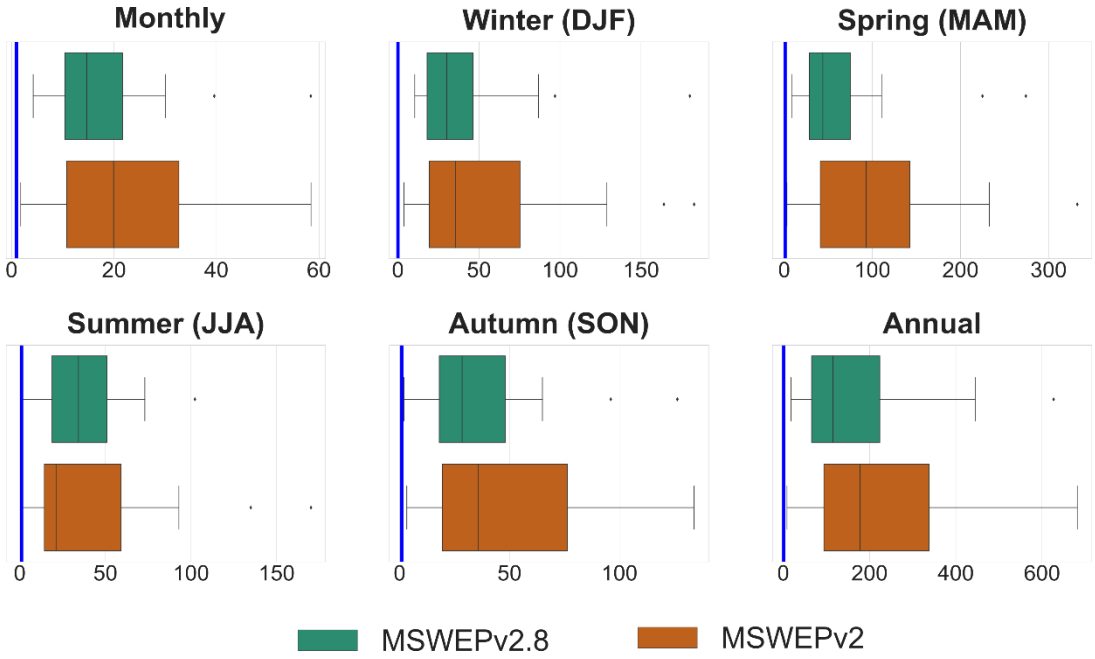

Figure S5. MAE for both MSWEP versions and precipitation gauge data at the corresponding grid cell for six temporal scales. The vertical blue line shows the optimum value for MAE.

48 **Table S1.** Precipitation products evaluated over Central Asia. NP: Near present.

Study	Evaluated datasets	Evaluated period	Evaluated temporal resolution	Product spatial resolution	Product temporal coverage	Product data sources	Region	Reference dataset	Source
Zandler et al. (2019)	GPCC Full data (2018)	1980–1994; 1998–2012	Monthly	0.25° x 0.25°	1891–2016	Gauge	Pamir Mountains, Tajikistan	5 gauging stations	Schneider et al. (2018a)
	GPCC Monitoring v.6			1° x 1°	1982–NP	Gauge			Schneider et al. (2018b)
	CRU TS 4.03			0.5° x 0.5°	1901–2018	Gauge			Harris et al. (2014)
	GPCP V2.3			2.5° x 2.5°	1979–NP	Satellite-Gauge			Huffman et al. (1997), Adler et al. (2018)
	PERSIANN-CDR			0.25° x 0.25°	1983–NP	Satellite			Ashouri et al. (2015)
	MERRA-2			0.5° x 0.625°	1980–NP	Reanalysis			Reichle et al. (2017)
	MERRA-2 Bias Corrected			0.5° x 0.625°	1980–NP	Reanalysis-Gauge			
	ERA-interim			0.7° x 0.7°	1979–NP	Reanalysis			Dee et al. (2011)
	ERA5			0.25° x 0.25°	1979–NP	Reanalysis			European Centre for Medium-range Weather Forecast (2019)

Study	Evaluated datasets	Evaluated period	Evaluated temporal resolution	Product spatial resolution	Product temporal coverage	Product data sources	Region	Reference dataset	Source
	TRMM 3B43 version 7	1998–2012		0.25° x 0.25°	1998–2014	Satellite			Huffman and Bolvin (2018)
Hu et al. (2018)	GPCC v 7	1901–2010	Monthly, seasonal, Annual	0.5° x 0.5°	1901–NP	Gauge	Kazakhstan, Uzbekistan, Turkmenistan, Kyrgyzstan, Tajikistan, and Xinjiang, China	586 meteorological stations: 438 CGP V1.0 (China Meteorological Administration, Global Precipitation V1.0) and 148 from NSIDC (U.S. National Snow and Ice Data Center)	Schneider et al. (2015)
	CRU TS 3.22			0.5° x 0.5°	1901–NP	Gauge			Harris et al. (2014)
	WM			0.5° x 0.5°	1901–NP	Gauge			Willmott and Matsuura (2012)

Study	Evaluated datasets	Evaluated period	Evaluated temporal resolution	Product spatial resolution	Product temporal coverage	Product data sources	Region	Reference dataset	Source
Guo et al. (2015);	TMPA 3B42V7	2004–2006	Daily, seasonal, monthly	0.25° x 0.25°		Satellite/ Satellite-Gauge	Kazakhstan, Uzbekistan, Turkmenistan, Kyrgyzstan and, Tajikistan	Asian Precipitation-Highly Resolved Observation Data integration Towards Evaluation of Water Resources (APHRODITE - 0.25° x 0.25°) Yatagai et al. (2012)	Huffman et al. (2007)
	CMORPH			0.25° x 0.25°		Satellite/ Satellite-Gauge			Joyce et al. (2004), Xie et al. (2014)
	GSMaP (MVK)			0.1° x 0.1°		Satellite/ Satellite-Gauge			Okamoto et al. (2005), Kubota et al. (2007), Mega et al. (2014)
	PERSIANN			0.25° x 0.25°		Satellite/ Satellite-Gauge			Sorooshian et al. (2000), Hsu et al. (1997), Ashouri et al. (2015)
Guo et al. (2017)	TMPA 3B42V7	2001–2006	Daily, seasonal	0.25° x 0.25°		Satellite/ Satellite-Gauge	Kazakhstan, Uzbekistan, Turkmenistan, Kyrgyzstan and, Tajikistan	APHRODITE - 0.25° x 0.25° Yatagai et al. (2012)	Huffman et al. (2007)
	CMORPH			0.25° x 0.25°		Satellite/ Satellite-Gauge			Joyce et al. (2004), Xie et al. (2014)

Study	Evaluated datasets	Evaluated period	Evaluated temporal resolution	Product spatial resolution	Product temporal coverage	Product data sources	Region	Reference dataset	Source
	GSMaP (RNL)			0.1° x 0.1°		Satellite-Reanalysis / Satellite-Reanalysis-Gauge			Okamoto et al. (2005), Kubota et al. (2007), Mega et al. (2014)
	PERSIANN			0.25° x 0.25°		Satellite/ Satellite-Gauge			Sorooshian et al. (2000), Hsu et al. (1997), Ashouri et al. (2015)
(Salehie et al., 2021)	APRHODITE	1979–2019	Monthly	0.25° x 0.25°		Gauge	Amu Darya Basin	55 meteorological stations	Yatagai et al. (2012)
	CHIRPS			0.05° x 0.05°	1981–NP	Satellite-Gauge-Reanalysis			Funk et al. (2015)
	CPC			0.5° x 0.5°		Gauge			https://psl.noaa.gov/data/gridded/data.cpc.globalprecip.html
	CRU TS V4.03			0.5° x 0.5°		Gauge			Harris et al. (2014)
	GPCC			0.5° x 0.5°		Gauge			Schneider et al. (2018b)
	PGF			0.25° x 0.25°		Gauge-Reanalysis			http://hydrology.princeton.edu/data/pgf/v3/0.25deg/daily/

Study	Evaluated datasets	Evaluated period	Evaluated temporal resolution	Product spatial resolution	Product temporal coverage	Product data sources	Region	Reference dataset	Source
	Udel V5.01			0.5° x 0.5°		Gauge			Willmott and Matsuura (2012)
Schär et al. (2004)	ERA-15	1979–1993	Monthly, Seasonal	2.5° x 2.5°	1979–1993	Reanalysis	Syr Darya and Amu Darya basins	4 meteorological stations	Gibson et al. (1999)
(Hu et al., 2016)	MERRA	1979–2010	Monthly, Seasonal, Annual	0.5° x 0.67°	1979–NP	Reanalysis	Kazakhstan, Uzbekistan, Turkmenistan, Kyrgyzstan, Tajikistan, and Xinjiang, China	199 meteorological stations	Rienecker et al. (2011)
	ERA-Interim			0.75° x 0.75°	1979–NP	Reanalysis			Dee et al. (2011)
	CFSR			0.31° x 0.31°	1979–NP	Reanalysis			Saha et al. (2010)
	TRMM 3B32			0.25° x 0.25°	1998–NP	Satellite			Huffman et al. (2007)
	MW			0.5° x 0.5°	1900–2010	Gauge			Willmott and Matsuura (2012)
(Malsy et al., 2014)	CRU TS 3.2	1971–2000	Mean monthly precipitation	0.5° x 0.5°	1901–2011	Gauge	Rivers Ob, Irtysh, Tobol, Ural, Amu Darya, Syr Darya, Tarim and the lakes Balkhash, Issyk	142 hydrological stations	Harris et al. (2014)
	GPCC v 6			0.5° x 0.5°	1901–2010	Reanalysis			Schneider et al. (2011)
	WATCH forcing data (WFD)			0.5° x 0.5°	1958–2001/1979–2009	Reanalysis			Weedon et al. (2014)

Study	Evaluated datasets	Evaluated period	Evaluated temporal resolution	Product spatial resolution	Product temporal coverage	Product data sources	Region	Reference dataset	Source
					(ERA Interim)		Kul, and Aral Sea		
	APRHODITE			0.25° x 0.25°	1951–2007	Gauge			Yatagai et al. (2012)
(Schiemann et al., 2008)	CRU TS 2.1	1960–1990	Monthly, seasonal, annual	0.5° x 0.5°	1901–2002	Gauge	Kazakhstan, Uzbekistan, Turkmenistan, Kyrgyzstan, and Tajikistan	CRU, GPCC, and UDEL	Mitchell and Jones (2005)
	GPCC			0.5° x 0.5°	1950–2000	Gauge			http://www.dwd.de/en/FundE/Klima/KLIS/int/GPCC/Projects/VASClimO
	UDEL 1.02			0.5° x 0.5°	1950–1999	Gauge			Legates and Willmott (1990)
	CAMS-OPI			0.5° x 0.5°	1979–2008	Gauge-Satellite			http://www.cpc.ncep.noaa.gov/products/global precip/html/wpage.camsopi.html
	ERA-40			~125 km	1958–2002	Reanalysis			(Uppala et al., 2005)

Study	Evaluated datasets	Evaluated period	Evaluated temporal resolution	Product spatial resolution	Product temporal coverage	Product data sources	Region	Reference dataset	Source
	NCEP			~210 km	1948–2008	Reanalysis			Kalnay et al. (1996)
	ECOP			(changing)	1985–2008	Reanalysis			http://www.ecmwf.int/products/data/operational system/
	CHRM			0.5° x 0.5°	1958–2001	Reanalysis			Vidale et al. (2003)
	CHRM-ECOP			0.5° x 0.5°	1997–2006	Gauge, Satellite			
(Lu et al., 2021)	SM2RAIN	2007–2019		0.125° x 0.125°	2007–NP		Kazakhstan, Uzbekistan, Turkmenistan, Kyrgyzstan, Tajikistan, and Xinjiang, China	SM2RAIN and ERA5	Brocca et al. (2019)
	ERA5			0.29° x 0.29°	1979–NP	Reanalysis			Hersbach et al. (2019)
	3B42			0.25° x 0.25°	1997–NP				Huffman et al. (2017)
	CHIRPS			0.05° x 0.05°	1981–NP	Satellite-Gauge-Reanalysis			Funk et al. (2015)
	CMORPH_CRT			0.0727° x 0.0727°	1998–NP				Joyce et al. (2004)

Study	Evaluated datasets	Evaluated period	Evaluated temporal resolution	Product spatial resolution	Product temporal coverage	Product data sources	Region	Reference dataset	Source
	GSMAP-Gauge			0.1° x 0.1°	2000–NP	Satellite, Gauge			Kubota et al. (2007)
	IMERG_FR			0.1° x 0.1°	2000–NP	Reanalysis			http://storm-pps.gsfc.nasa.gov/storm
	PERSIANN_CDR			0.25° x 0.25°	1983–NP	Satellite			Sorooshian et al. (2000)

Table S2. Local gauging stations used in the validation. KG: Kyrgyzstan; KZ: Kazakhstan; TM: TJ: Tajikistan; Turkmenistan; UZ: Uzbekistan. (–) Not available. (––) Not used. * Based on information provided by ftp://chg-ftpout.geog.ucsb.edu/pub/org/chg/products/CHIRPS-2.0/list_of_stations_used/monthly. These stations are also considered independent for MSWEP.

Station	Country	Altitude (m)	Lat	Lon	Annual precipitation (mm/year)	Available period (monthly)	Available period (daily)	Period used in CHIRPS*	Validation period
Ak-Terek	KG	1,190	40.37	74.22	1085	2000–2015	–	––	2000–2015
Baytyk	KG	1,579	42.67	74.63	559	2000–2015	–	1981 –2000	2001–2015
Buhara	UZ	219	39.72	64.62	126	–	1988–2012	1981–1995/ 2000–2020	1995–1999
Bulunkul	TJ	3,744	37.70	72.95	88	1981–1990/1999–2013	1936–1967/1975–1989	1981–1991	1999–2013
Chatkal	KG	2,300	41.82	71.10	500	2000–2015	–	1981–1995	2000–2015
Gulcha	KG	1,575	40.30	73.47	678	2000–2015	–	1981–1997	2000–2015
Guzar	UZ	527	38.62	66.27	200	–	1988–2001/2005–2012/2015–2016	1981–1999	2005–2012
Humragi	TJ	1,737	38.28	71.33	169	1958–1994/2001–2008	1936–1970/1976–1984	––	1981–1994/2001–2008

Station	Country	Altitude (m)	Lat	Lon	Annual precipitation (mm/year)	Available period (monthly)	Available period (daily)	Period used in CHIRPS*	Validation period
Irkht	TJ	3,276	38.13	72.62	120	1981–1991/1998–2009	1939–1967/1974~1985	1981 – 1997 / 2014–2020	1998–2009
Ishkashim	TJ	2,510	36.72	71.61	134	1981–1991/1998–2009	1939–1967/1974–1985	1981–1991 / 2014–2020	2001–2009
Javshangoz	TJ	3,438	37.36	72.44	87	1981–1995/2001–2006/2009–2013	1936–1989	1981–1991	1992–1994/2001–2006/2009–2013
Kala-i-Khumb	TJ	1,231	38.51	70.94	485	1997–2005	1936–1981	1981–1991 / 2013–2020	1997–2005
Kara Kuzhur	KG	855	41.93	76.30	264	2000–2015	–	1981–1991	2000–2015
Karshi	UZ	363	38.75	65.72	255	–	1988–1999/2007/2014–2018	1981–1992/2000–2020	1993–1999
Khorog	TJ	2,077	37.48	71.54	272	1936–2001–2013	1939–1989/2001–2013	1991–2020	1981–1990
Kyzyl-Adyr	KG	1,764	42.62	71.59	327	2000–2015	–	1981–1991	2000–2015
Lasi_Uzgen	KG	978	40.77	73.30	977	2000–2015	–	1981–1991	2000–2015
Minchukur	UZ	2,147	38.65	66.93	676	–	1988–1992/1994–2013/2015–2016	1981–1999	2000–2013

Station	Country	Altitude (m)	Lat	Lon	Annual precipitation (mm/year)	Available period (monthly)	Available period (daily)	Period used in CHIRPS*	Validation period
Murghab	TJ	3,576	38.15	73.96	80	1936–1991–1993/1998–2009	1936–1970/1974–1985	1981–1993 / 2013–2020	1998–2009
Navabad	TJ	2,576	37.67	71.83	392	1981–2013	1956–1989	––	1981–2013
Navoi	UZ	339	40.13	65.20	176	–	1988–2017	1981–1995/2009–2019	1996–2008
Oygaing	UZ	1,620	42.00	70.63	733	2000–2015	–	1981–1999	2000–2015
Rushan	TJ	1,980	37.95	71.57	289	1960–2001–2008	1936–1984/2001–2008	1981–1991/2013–2020	2001–2008
Savnob	TJ	2,955	38.40	72.60	153	1986–1999–2001–2005	1962–1981	––	1986–2005
Shahrisabz	UZ	1,026	39.25	67.07	499	–	1988–2018	1985–1999	2000–2018
Shaymak	TJ	3,840	37.54	74.82	151	1981–1991/1999–2009	1936–1970/ 1975–1985	1981–1991	1999–2009
Shelek	KZ	600	43.60	78.25	274	2000–2015	–	1981–1991/ 2018–2020	2000–2015
Tahtamish	TJ	3,729	37.83	74.64	68	1968–1987	1944–1964	––	1981–1987

Station	Country	Altitude (m)	Lat	Lon	Annual precipitation (mm/year)	Available period (monthly)	Available period (daily)	Period used in CHIRPS*	Validation period
Takhta Bazar	TM	354	35.97	62.91	216	2000–2015	–	1981–1991	2000–2015
Zhalanash	KZ	1,690	43.04	78.64	507	2000–2015	–	––	2000–2015

Eq. S1

$$KGE' = 1 - \sqrt{(r-1)^2 + (\beta-1)^2 + (\gamma-1)^2}$$

$$r = \frac{1}{n}\sum_{1}^{n} \frac{(O_n - \mu_o) * (S_n - \mu_s)}{\sigma_o * \sigma_s}$$

$$\beta = \frac{\mu_s}{\mu_o}$$

$$\gamma = \frac{CV_s}{CV_o} = \frac{\sigma_s/\mu_s}{\sigma_o/\mu_o},$$

where μ is the distribution mean, σ is the standard deviation, and o and s are the observed values and the product estimates, respectively.

Eq. S2

$$MAE = \frac{1}{N}\sum_{i=1}^{N} |s_i - o_i|$$

Eq. S3

$$POD = \frac{hits}{hits + misses}$$

$$FAR = \frac{false\ alarms}{hits + false\ alarms}$$

$$fBIAS = \frac{hits + false\ alarms}{hits + misses}$$

Eq. S4

$$PKi = \frac{Pi}{PA},$$

where *PKi* is the Pardé coefficient of month *i*, *Pi* is the mean monthly precipitation (averaged over the study period) in month *i*, and *PA* is the mean annual precipitation (averaged over the same years) (Parajka et al., 2008, Weingartner et al., 2013).